UCRL-LR-134107

The Scrounge-atron

A Proton Radiography Demonstration Accelerator

Owen J. Alford, Peter D. Barnes, Jr., Anthony K. Chargin,
Edward P. Hartouni, Jeffrey N. Hockman,
Thomas L. Moore, Randy E. Pico
Lawrence Livermore National Laboratory

Alessandro G. Ruggiero
Brookhaven National Laboratory

December 18, 1998

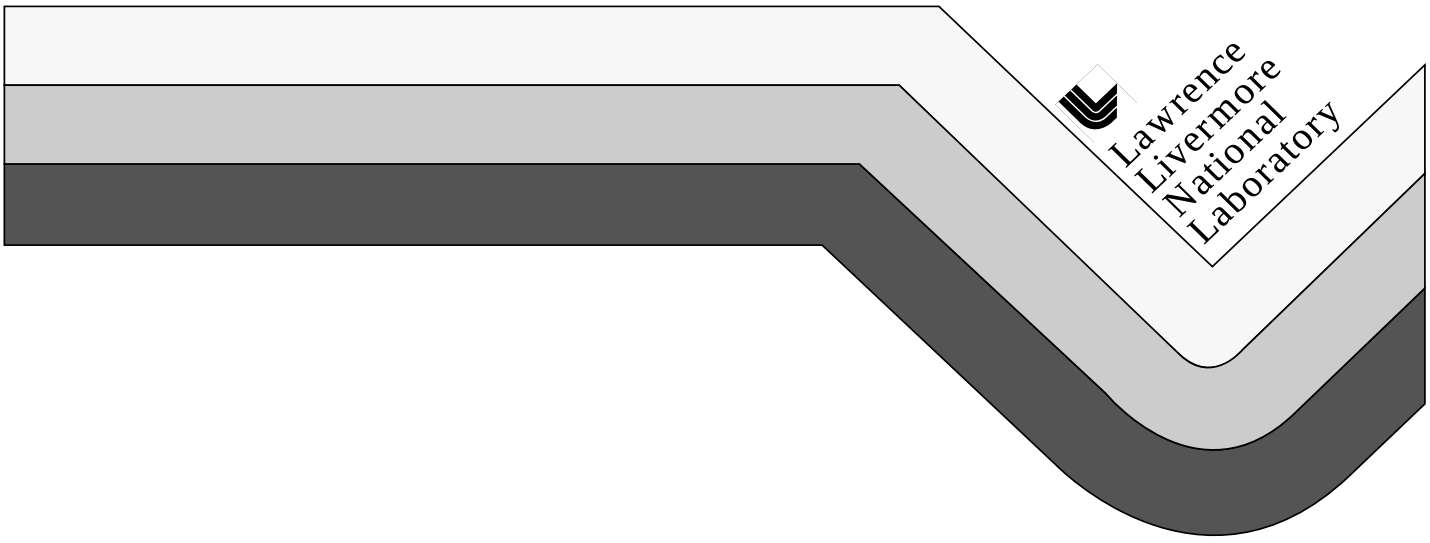

Work performed under the auspices of the U.S. Department of Energy by Lawrence Livermore National Laboratory under Contract W-7405-ENG-48.

UCRL-LR-134107

The Scrounge-atron

A Proton Radiography Demonstration Accelerator

Owen J. Alford, Peter D. Barnes, Jr., Anthony K. Chargin,
Edward P. Hartouni, Jeffrey N. Hockman,
Thomas L. Moore, Randy E. Pico
Lawrence Livermore National Laboratory

Alessandro G. Ruggiero
Brookhaven National Laboratory

December 18, 1998

LAWRENCE LIVERMORE NATIONAL LABORATORY
University of California • Livermore, California • 94550

The Scrounge-atron

A Proton Radiography Demonstration Accelerator

Owen J. Alford, Peter D. Barnes, Jr., Anthony K. Chargin,
Edward P. Hartouni,* Jeffrey N. Hockman,
Thomas L. Moore, Randy E. Pico
Lawrence Livermore National Laboratory

Alessandro G. Ruggiero
Brookhaven National Laboratory

December 18, 1998

Abstract

The Scrounge-atron is a concept that could provide a demonstration accelerator for proton radiography. As discussed here, the Scrounge-atron would be capable of providing a 20 GeV beam of ten pulses, 10^{11} protons each, spaced 250 ns apart. This beam could be delivered once every minute to a single-axis radiographic station centered at the BEEF facility of the Nevada Test Site. These parameters would be sufficient to demonstrate, in five years, the capabilities of a proton-based Advanced Hydrotest Facility, and could return valuable information to the stockpile program, information that could not be obtained in any other way. The Scrounge-atron could be built in two to three years for $50–100 million. To meet this schedule and cost, the Scrounge-atron would rely heavily on the availability of components from the decommissioned Fermilab Main Ring.

* To whom correspondence should be addressed: hartouni1@llnl.gov

Table of Contents

Abstract ..... *i*
Table of Figures ..... *v*
Table of Tables ..... *v*

Introduction **1**

Experimental Program **3**

Design Requirements **3**

Machine Description **6**

- **Ring Lattice** **7**
- **Injector Linac** **13**
- **Injection, Extraction, Transport, and Beamstops** **15**
- **Radiography Beamline** **18**
- **Magnet System** **19**
- **Other Systems** **24**
- **Civil Engineering, Enclosures, and Radiation Shielding** **26**

Scrounging Fermilab **27**

Schedule **28**

Cost **29**

Energy, Intensity, and Beamline Upgrades **32**

- **Energy Upgrade** **32**
- **Intensity Upgrade** **33**
- **(Nearly) Arbitrary Pulse Formats** **33**
- **Beamline Upgrade to the AHF** **33**

Recommendations for Future Work **34**

Conclusion **35**

References **35**

Table of Figures

Figure 1. Resolution Due to Exit Window Coulomb Scattering. 4
Figure 2. Beam Attenuation. 5
Figure 3. Scrounge-atron Facility Plan 7
Figure 4. Lattice Cell Structure. 9
Figure 5. Injection and Extraction Straights. 9
Figure 6. Reference Trajectory and Injection Beam Envelope in a Dipole. .11
Figure 7. Lattice Functions. 12
Figure 8. The Injection Linac. 14
Figure 9. Beam Time Structure. 15
Figure 10. Linac to Ring Transport and Injection. 16
Figure 11. Extraction and Extraction Transport Line. 17
Figure 12. Radiography Beamline from Diffuser to Beam Stop. 19
Figure 13. Ring Power Supply Busing. 21
Figure 14. Magnet Raft Components. 22
Figure 15. Scrounge-atron Enclosure. 27
Figure 16. Scrounge-atron at BEEF. 28
Figure 17. Technically Driven Construction Schedule. 30
Figure 18. Scrounge-atron and the AHF. 34

Table of Tables

Table 1. Design Requirements for the Scrounge-atron 3
Table 2. Fixed Parameters. 8
Table 3. Energy Dependent Parameters. 13
Table 4. Injection Linac Parameters. 14
Table 5. Dipole and Quadrupole Electrical Properties. 20
Table 6. Magnet Types and Quantities. 23
Table 7. Fixed rf Parameters. 24
Table 8. Varying rf Parameters at Injection and Extraction. 24
Table 9. Site-wide Power Requirements. 29
Table 10. Work Breakdown Structure and Cost Estimate. 31
Table 11. Energy Upgrade Parameters. 32

Introduction

In the Comprehensive Test Ban Treaty era, no nuclear weapons tests are allowed. To continue to certify the safety and reliability of the U.S. nuclear weapons stockpile, the weapons complex will require a major new radiographic facility, the Advanced Hydrotest Facility (AHF), to be built circa 2008.[1] This facility will provide multiple radiographic pulses on multiple axes. One of the two radiographic probes under consideration is a high-energy proton beam.

The use of high-energy protons for radiography was suggested by Los Alamos National Laboratory (LANL) following tests of the concept at low energy in 1995.[2] Proton radiography at high energy was considered problematic due to the effects of multiple Coulomb scattering in the objects being radiographed. This scattering causes shadow radiographs to be blurred. The LANL concept was to use a set of magnetic lenses to focus the scattered protons onto an image plane. Detectors placed at this image plane would record a radiographic image of the object with the multiple Coulomb scattering essentially eliminated. Proton radiographic probes are of interest to the AHF because the proton interaction lengths are a good match to the areal densities of the objects being radiographed. In addition, protons produce a small number of secondary particles in the interactions. These secondary particles, which are potential backgrounds for radiography, are further reduced by the magnetic lens systems used to produce the radiographic images. The detection of protons is usually very efficient (due to the proton's charge), allowing thin detectors to be used. The protons have minimal interactions in the thin detectors, which allows proton radiography to use multiple detector systems (and multiple lenses), thus increasing the radiographic information obtainable from the object.

Since there is almost no experience with protons as radiographic probes, it would be extremely valuable to perform a series of demonstration experiments to develop the tools, techniques, and understanding that will be required to determine if protons should be the radiographic probe for the AHF, and, if that decision were made, to have the expertise to design a proton-based AHF. These experiments should provide information on a number of hydrotest topics relevant to Science-Based Stockpile Stewardship and should use appropriate objects and materials, including classified experiments and high-explosives-driven dynamic experiments. The experimental program is discussed in a later section. The radiographic requirements of these experiments determine the proton accelerator performance requirements, which are modest. However, currently there exist no suitable facilities in the United States to perform these experiments, due to classification, material, or other safety issues.

The purpose of the research leading up to this report is to determine whether it is possible to build a 20 GeV proton synchrotron suitable for the experimental program (a) as quickly as possible, that is in two or, at most, three years and (b) as economically as possible, that is for a price in the $50–100 million range.

The result of this research is that, indeed, such a machine is technically feasible and can be built within the cost and schedule constraints. To meet the schedule and cost goals, this machine relies heavily on the availability of components from the decommissioned

Fermi National Accelerator Laboratory (Fermilab) Main Ring. Since the operation has been called “scrounging Fermilab equipment,” we refer to the project as the “Scrounge-atron.”

We can meet the schedule and cost goals by adopting the following design procedure: (1) use existing parts where available and appropriate; if parts are not available, (2) use existing designs; and only if these are not available, (3) design and construct the required part. This procedure minimizes the total amount of design for the accelerator. This approach is possible because, for most of the accelerator systems, the characteristics required for radiography are far below the current state-of-the-art used in new accelerators.

The decommissioning of the Fermilab Main Ring has made a large variety of parts available for reuse. The Scrounge-atron is designed around the B1-type dipole magnets and the Q4-type quadrupole magnets. Correcting sextupole, octupole, and regular and skew quadrupole magnets are also available. The vacuum pipes are epoxied into the dipoles and quadrupoles, so only short sections are required between the magnets in the Scrounge-atron. All of the required power supplies are available. Most of the diagnostic equipment is available, such as beam position monitors, which are integrated into the quadrupole vacuum pipes, and the associated readout electronics. An ion source and radio-frequency quadrupole (RFQ) parts are available, as are the Princeton-Penn Accelerator (PPA) radio-frequency (rf) cavities, modulators, and power supplies. There are even electrical utility substation components and cooling water heat exchangers available. Unfortunately, all steering dipoles have been reused in the Main Injector, so steering dipoles for the Scrounge-atron have to be built, but not entirely from scratch—the Main Injector or Main Ring designs are perfectly adequate, and the tooling exists at Fermilab. The only other major ring components that will have to be built are 62 quadrupoles, since only 40 exist. Again, the design and tooling exist.

Many of the major linac components are also available, including the ion source (Brookhaven National Laboratory [BNL]), parts of the RFQ (Lawrence Berkeley National Laboratory [LBNL] design), and the second section of drift tube linac (Fermilab). Designs exist for the two remaining components, the first drift tube linac section (BNL/Fermilab design), and additional cavity-coupled linac (CCL) cavities (Fermilab design).

As discussed here, the Scrounge-atron will use these components to provide a 20 GeV beam of ten bunches (or frames), 10^{11} protons each and 20 ns duration, spaced 250 ns apart. This beam will be delivered once every minute to a single-axis radiographic station centered at the Big Explosive Experiment Facility (BEEF) facility of the Nevada Test Site. These parameters are sufficient to demonstrate, in five years, the potential capabilities of a proton-based AHF, as well as return valuable information to the stockpile program that can not be obtained in any other way.

If, as we expect, protons are a suitable radiographic probe, there is a natural upgrade path from the Scrounge-atron to the full AHF capabilities, allowing a staged approach to the final facility. It is possible with only minor modifications to accelerate and extract the proton beam at 40, and maybe even 50 GeV, if this should be required. With a more advanced kicker magnet it will also be possible to extract one proton bunch at a time and achieve a nearly arbitrary frame spacing over a much longer time interval. The addition of a small rapid cycling booster will increase the proton beam intensity by an order of magnitude, if this should be required. A large external collector ring adds the capability to simultaneously extract several beam bunches along multiple axes.

Considering its nature, this research is by no means meant to be a proposal for construction. Though the results are definitely encouraging, and no showstoppers have been found, this work has been done in a short period of time and with limited effort. A more detailed study leading to a conceptual design report should be undertaken. There are a

relatively few areas in which concentrated effort would have significant impact in reducing the cost and schedule uncertainty. The most significant issues are the injection field and sagitta and the choice of a linac or linac plus booster for the injector. These are discussed at the end of this report.

To summarize, the Scrounge-atron is a demonstration accelerator for proton radiography. It will provide a 20 GeV beam of ten pulses, 10^{11} protons each, spaced 250 ns apart. This beam will be delivered once every minute to a single-axis radiographic station centered at the BEEF facility of the Nevada Test Site. These parameters are sufficient to demonstrate, in five years, the capabilities of a proton-based Advanced Hydrotest Facility. The Scrounge-atron can be built in two to three years for $50–100 million, by using components from the decommissioned Fermilab Main Ring. Finally, the Scrounge-atron will begin returning valuable science many years earlier and at a fraction of the initial cost of the full AHF.

The remainder of this report discusses the experimental program, design requirements, a detailed description of the machine, a first cut at the schedule and cost, and conclusions.

Experimental Program

The experimental program to be performed at a Scrounge-atron facility begins with a simple extension of relevant hydrotest experiments (such as those performed at the LLNL FXR (Flash X-Radiography) facility and the LANL PHERMEX (Pulsed High-Energy Radiographic Machine Emitting X-rays). These experiments will exploit the framing capability of the beam to produce “movies” of the various hydrotests. As these experiments progress, more elaborate analyses utilizing precision density determination and material identification will be possible. Further understanding of the hydrotest dynamics can be obtained by extending the extraction capabilities of the Scrounge-atron to allow essentially random pulse formats.

Design Requirements

The design parameters for the Scrounge-atron are set by the experimental program requirements.[1] These parameters are related to image spatial resolution, statistical variance of the image on a pixel-by-pixel basis, number of time frames and duration of frame, and repetition rate of the machine. The design requirements are shown in Table 1.

Table 1. Design Requirements for the Scrounge-atron.

Parameter	**Value**	**Unit**
Final Energy	20	GeV
Repetition Period	1	min
Number of Proton Bunches	10	bunches
Bunch Separation	250	ns
Number of Protons / Bunch	10^{11}	protons
Total Number of Protons/pulse	10^{12}	protons

The desired spatial resolution, Δ, is less then 1 mm FWHM (full width at half maximum). This resolution, sufficient to identify image features of interest to the experimental program, is determined by multiple Coulomb scattering (MCS) in the beamline window located just downstream of the object. MCS in this window introduces image blur

(whereas MCS in the upstream window and in the object do not contribute to this blur). The root-mean square (rms) scattering angle can be approximated by the expression

$$\theta_0 = \frac{13.6\ \text{MeV}}{\beta cp}\sqrt{\frac{x}{X_0}}\left[1 + 0.038\ln\left(\frac{x}{X_0}\right)\right], \tag{1}$$

where p is the proton momentum, x the path length through the window, and X_0 the radiation length of the window material. The spatial resolution at the object can be approximated by

$$\Delta(FWHM) = 2.36\, l\theta_0, \tag{2}$$

where l is the distance from the object position to the window. The resolution improves as the beam momentum increases. Figure 1 shows the resolution for windows of various thickness and material located 1 m away from the object.

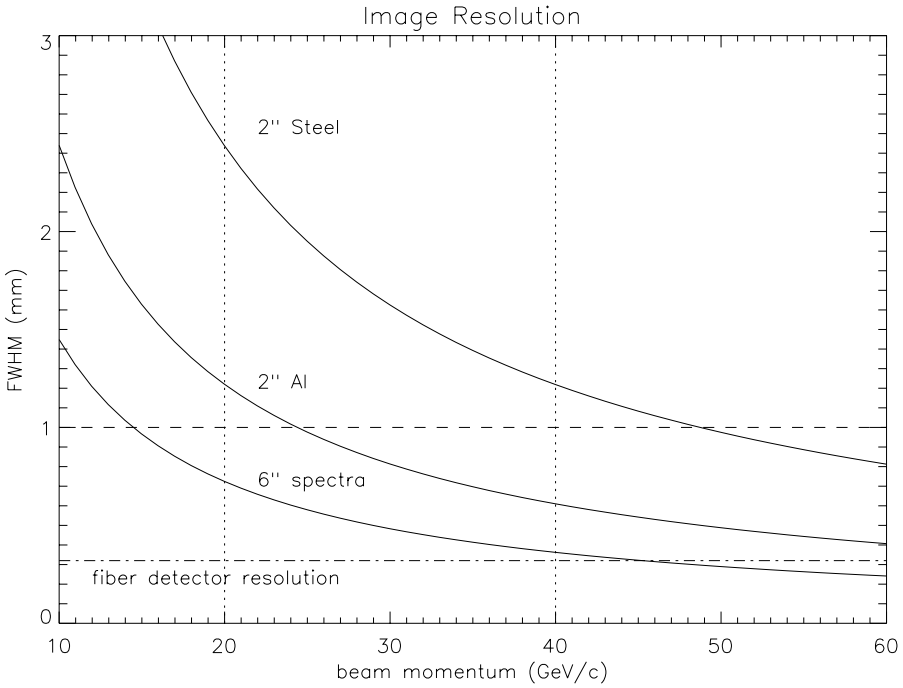

Figure 1. Resolution Due to Exit Window Coulomb Scattering.
The expected spatial resolution as a function of momentum for steel, aluminum, and Spectra carbon fiber composite windows located 1 m downstream of the object. The required resolution is 1 mm. The minimum resolution is set by the detector system, assumed here to have 0.25 mm diameter scintillating fibers.

An assumption of the design is that the windows would mitigate shrapnel and blast shock wave but would not need to guarantee confinement of the experiment. This allows aluminum windows to be used, or possibly a composite material like Spectra. Using these materials reduces the required beam momentum needed to achieve a specific image resolution. The beam momentum of the Scrounge-atron is chosen to be 20 GeV/*c*.

The intensity requirement for a single image is set by the area of the imaging array and the approximate attenuation of the beam pulse through the object and the other material

in the beamline. Taking a 10 cm × 10 cm field of view and a detector at the image plane with 0.250 mm × 0.250 mm pixels results in 1.6×10^5 imaging elements. To obtain a 1% intensity measurement for a pixel requires roughly 1×10^4 protons per pixel or 2×10^9 protons at the image plane. The proton beam intensity decreases exponentially in passing through material. This can be expressed by the relationship

$$\frac{I}{I_0} = e^{-l\rho/\Lambda}, \tag{3}$$

where l is the path length through the material, ρ is the material density, and Λ is the attenuation constant,

$$\Lambda = \frac{A}{N_0 \sigma}, \tag{4}$$

where A is the atomic mass of the material, N_0 is Avogadro's number, and σ is the proton absorption cross section. Figure 2 shows the attenuation fraction for elements from H to U over the ρl range of interest.

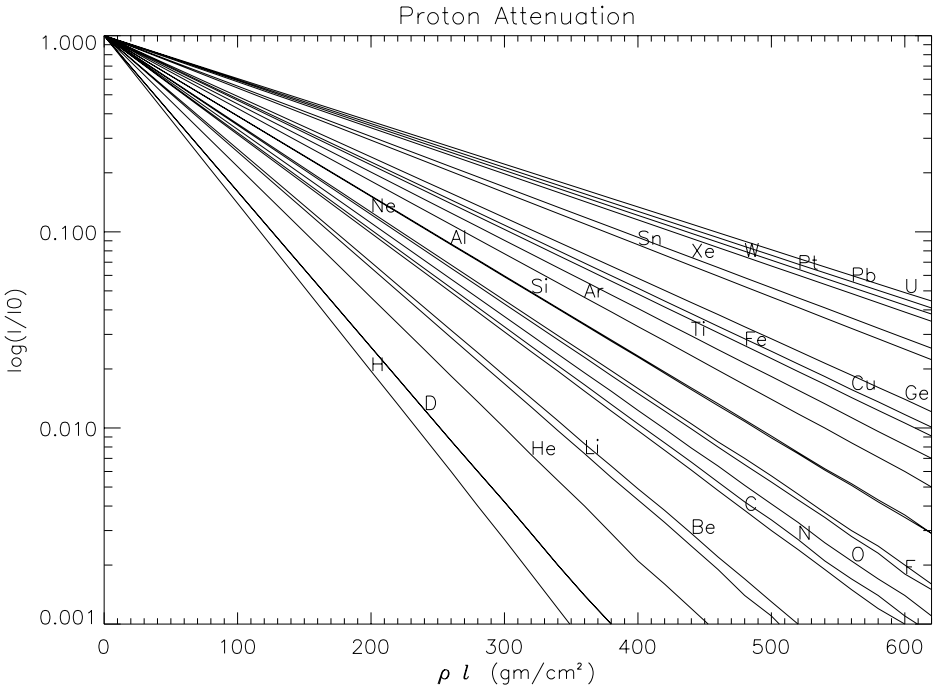

Figure 2. Beam Attenuation.
Attenuation as a function of ρl for elements from H to U.

For the purpose of estimating beam intensities, we will take the total attenuation of protons through the beamline windows and object to be of order 0.1-0.01. To obtain 2×10^9 protons at the image plane would require of order 10^{10} to 10^{11} incident protons per beam pulse.

The number of beam bunches or frames required for dynamic radiography can only be chosen based on experimental considerations. Currently no radiography facility provides more than two frames on a μs time scale. We choose to provide 10 bunches, spaced 250 ns

apart, with a 12 ns bunch width. These parameters are compatible with the AHF requirements. The simplest extraction scheme has the entire beam extracted in one turn, *i.e.*, with 10 bunches equally spaced in time. The 10 frames would then span 2.5 μs. With more complex extraction schemes, a single bunch might be extracted at an arbitrary time allowing a variation in the frame time format spanning hundreds of microseconds.

With 10 bunches, the total intensity required in the Scrounge-atron is roughly 10^{12} protons. The number and spacing of the bunches also set a minimum circumference of the machine, 750 m.

The maximum rate at which the beam should be delivered to the object is set by the detector data-download time. For current charge-coupled device (CCD) camera systems this time is of order minutes. Even assuming improvements in electronics and camera systems it seems unlikely that radiography experiments would require beam cycle times more rapid than once per minute. The accelerator repetition rate requirement is set by the needs of machine "tuning" rather than by the radiographic requirements.

Based on this discussion, the machine design requirements are shown in Table 1.

Machine Description

Figure 3 shows the Scrounge-atron layout. It consists of a 300 MeV injector linac, the linac-to-ring transfer line (LTRT), the 20 GeV synchrotron, the ring-to-radiography transport line (RTRT), and the radiography beamline. The main parameters of the Scrounge-atron are given in Table 2. These are roughly $1/10^{th}$ the values of the Fermilab Main Ring. Therefore, we should expect that the Scrounge-atron will look like roughly one-tenth of the Main Ring.

The synchrotron has a periodicity of two, with a reflection symmetry within the period. Each period contains a long arc, which together account for 78% of the ring. The arcs are joined together by two insertions, on opposite sides of the ring. Injection equipment, extraction equipment, and the accelerating cavities are in one of the insertions in the transfer enclosure on the linac side of the ring. All accelerator components can be transported into the tunnel enclosure through either the transfer enclosure or through alcoves at the other insertion and in the middles of the arcs. Ten major power supply utility substations are located around the ring; eight serve the synchrotron proper, and two serve the LTRT and the RTRT. The linac is housed in a separate enclosure, which includes the klystron gallery.

The beam is transported to the firing site through the RTRT beamline. At the firing site the beam enters a radiography beamline, consisting of a diffuser, matching lens, intensity measurement station, first imaging lens, blast protection bullnoses around the object location, and two consecutive imaging lenses with collimators and measurement stations. The object is located in a pit slightly offset from the center of the BEEF firing site. When BEEF is used without the Scrounge-atron, shielding blocks cover the object pit. For radiography shots, the pit is opened up, allowing easy installation of the object and open air firing. At either end of the pit, bullnoses protect the upstream and downstream beamline components and enclosures.

The major civil construction consists of the linac enclosure, 100 m long; the ring enclosure, 910 m long; the transfer line to the firing site, 120 m long; and the radiography beamline at the firing site, 100 m long.

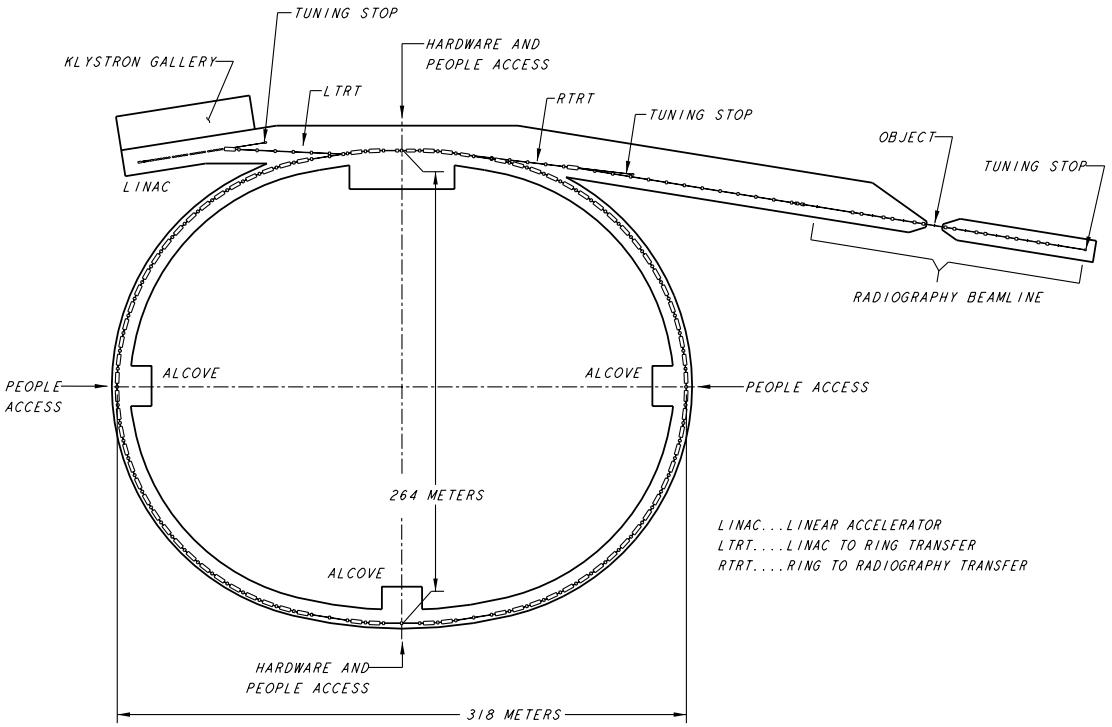

Figure 3. Scrounge-atron Facility Plan

Ring Lattice

The lattice parameters of the ring are given in Table 2. The total lattice is made of a continuous sequence of 46 identical FODO cells,* as shown in Figure 3. The lattice has a periodicity of two, each superperiod with a mirror symmetry. Each period consists of 20 identical bend cells ("**C**") with ~60° betatron phase advance, and three "empty cells" ("**CE**") with the dipoles removed. A **C** and **CE** cell are shown in Figure 4. The use of a single cell with 60° phase advance results in a very uniform and completely matched lattice without requiring any special magnets. The **CE** cells in the transfer enclosure provide space for injection, extraction and rf devices. Identical empty cells are required on the other side of the ring for closure; these are left empty, as shown in Figure 5.

The structure of a period is then as follows (in SYNCH notation):

```
.PER      BML     // C  C  C  C  C  C  C  C  C
                  //    CE C  CE C  CE
                  // C  C  C  C  C  C  C  C  C          (5)
```

A single bending magnet ("**B**") is located in each half cell. The structure of a regular cell ("**C**") is then

```
.C        BML     // QF O  B  O  QD QD O  B  O  QF      (6)
```

* The basic repeating cell of a synchrotron lattice consists of a focusing ("**F**") quadrupole, a drift length or dipole "**O**," a defocusing ("**D**") quadrupole, and a final drift length or dipole "**O.**" Figure 4 shows two cells, one with dipoles and one without.

Table 2. Fixed Parameters.

Parameter	Value	Units
Lattice		
Periodicity	2	
# Straight Cells "CE"/ Period	3	
# Bend Cells "C"/ Period	20	
Cell Length	19.786	m
Ring Circumference	910.138	m
B1 Type Dipoles		
Aperture (H x V)	5 x 1.5	in^2
Length	6.071	m
Bending Angle	78.540	mrad
Bending Radius	77.313	m
Sagitta	59.606	mm
Ramp Rate	2.000	kG/s
Number of Dipoles	80	
Q4 Type Quadrupoles		
Aperture (H x V)	5 x 2	in^2
Length	1.321	m
$B'/B\rho$	0.0779	m^{-2}
Ramp Rate	12.045	kG/m s
Number	92	
Drifts		
Short "O"	1.251	m
Long "D"	8.572	m
Accelerator Functions		
Phase Advance / Cell	61.2	°
β_{max} - max	34.072	m
η_{max} - max	3.762	m
γ_T - Transition	7.387	
Tune		
Q_h - Horizontal Tune	7.82	
Q_v - Vertical Tune	7.80	
ξ - Chromaticity	-1.11	

and that of an empty cell ("**CE**") is

```
.CE        BML      // QF      D       QD QD      D       QF          (7)
```

Note that a QF (QD) horizontally focussing (defocusing) quadrupole is half of the physical quadrupole length given in Table 2, so that the sequence QD QD stands for a complete physical quadrupole. ("**C**" and "**CE**" are the basic elements of the period structure, so that the QF at the end of a cell is immediately followed by a corresponding QF at the beginning of the next cell, thus resulting in a single physical quadrupole.) This convention allows us to determine the beam parameters at the center of the quadrupoles, where they are maximum. The cell structure is illustrated in Figure 4.

Injection Energy and Space Charge

The injection energy of 300 MeV into the synchrotron is set by two main parameters. First is the minimum usable field of the Fermilab dipoles. A higher injection field requires a

larger injection energy, hence driving up the cost of the linac. Similarly, the beam transverse dimension in the presence of space charge, coupled with the beam sagitta and the magnet aperture, argues for higher injection energy, again driving up the linac cost.

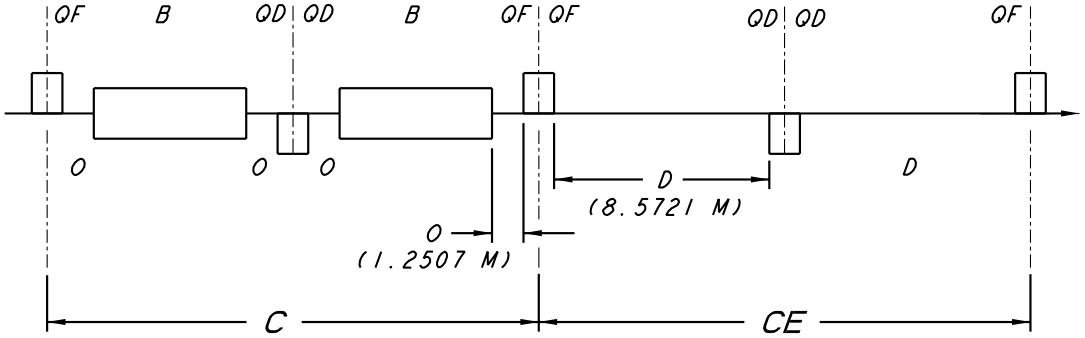

Figure 4. Lattice Cell Structure.
Cell structure in accelerator notation. The horizontal line represents the beam trajectory. Boxes above (below) the line are horizontally focussing (defocusing) quadrupoles. Boxes centered on the line are dipoles. On the left is a "**C**" bend cell, followed by a "**CE**" empty (straight) cell.

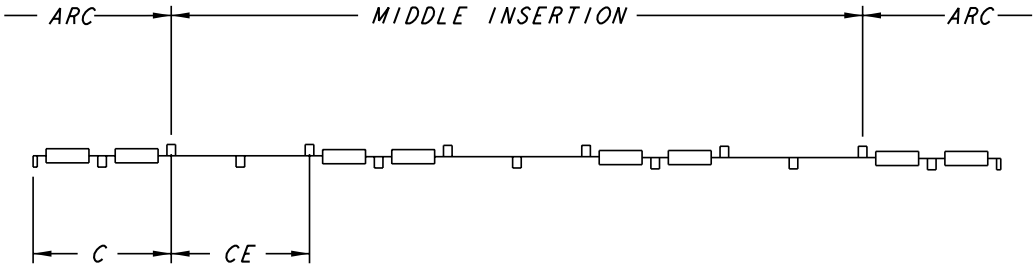

Figure 5. Injection and Extraction Straights.

The Fermilab Main Ring successfully operated for much of its life with an injection field of 400 G for the 8 GeV beam from the 15-Hz Booster.[3] However, in the early years the Booster only delivered a 7 GeV beam, with a corresponding 350 G field in the Main Ring. We have adopted this lower value as the minimum injection field in the Scrounge-atron, which implies a 300 MeV injection energy. The Main Ring had a more complicated injection cycle than the Scrounge-atron, with a front porch of 0.8 s for the injection in boxcar fashion of multiple pulses from the Booster. The Scrounge-atron does not need a front porch since the beam is injected in a single turn on the fly during the linear magnetic field ramp. This makes the injection process less sensitive to magnetic field errors, which are the primary concern in operating at low injection field. On balance, then, the Scrounge-atron uses the dipoles at a proven injection field and in a less sensitive operation mode than the Main Ring.

Space-charge effects become progressively more severe at low energy, causing the beam size to grow. The beam size should be small enough to pass through the physical aperture of the Fermilab bending magnets. Because of space charge, the beam full emittance, ε, which sets the physical beam size, is determined by the beam intensity, N_p, energy (through the relativistic factors β and γ), and the allowed tune shift, $\Delta\nu$, by the formula:

$$\varepsilon = \frac{N_p r_p b}{2\beta^2\gamma^3\Delta\nu}, \tag{8}$$

where r_p is the classical radius of the proton, and b is the bunching factor, the ratio of peak beam current to average current. Large tune shifts make it more likely that some beam will be lost due to resonances. Here we assume the conservative value 0.2. Using a bunching factor of 4, we compute a full beam emittance (both horizontal and vertical) of $\varepsilon = 5\ \pi$ mm mrad. The corresponding normalized emittance is $\varepsilon_n = \varepsilon\beta\gamma = 4.3\ \pi$ mm mrad. With the synchrotron lattice described earlier the full beam size in the dipole magnets is ±12.0 mm vertically and ±12.4 mm horizontally.

Circumference

The field and injection energy determine the size of the ring. Given the 350 G bending field at 300 MeV injection energy, the bending radius is ρ = 77.313 m. Allowing sufficient space on both sides of the quadrupoles (1.251 m for correcting magnets, beam position monitors, vacuum ports, bellows, and flanges), the packing factor in the arcs is 62%. There are also a total of six empty cells for injection, extraction, and rf cavities, resulting in a total circumference of 910.138 m.

Dipole Type and Sagitta

The Fermilab Main Ring was made of 774 bending magnets: 378 of the B1-type (5×1.5 in.^{2} = 127×38 mm^2 internal aperture) and 396 of the B2-type (4×2 in.^{2} = 102×51 mm^2).[4] The two types are the same length (239 in. = 6.0706 m) and are straight and rectangular.

When operated at 200 GeV the Main Ring dipole field was 9 kG to give a bending angle per dipole of 8.12 mrad. Because of the small bending angle, the sagitta was small, 6.2 mm, so there was no need to physically curve the dipole magnets. The Scrounge-atron at 20 GeV requires about the same bending field in its 80 dipoles. Because of the fewer number of dipoles, the bend angle is significantly larger, 78.54 mrad, and the trajectory is significantly curved, with a 59.6 mm sagitta. (*Sagitta* is the largest distance between an arc and the straight line connecting the endpoints of the arc. If the sagitta is larger than the width of the dipole aperture, then the curved beam trajectory will hit the wall of the magnet.) This is probably the most interesting accelerator physics issue in the project. Because of the trajectory sagitta, we have chosen the B1-type dipoles for their larger width despite the narrower gap. The B1 dipole parameters are listed in Table 2. Including the vacuum chamber thickness, the actual physical horizontal aperture is 121 mm, of which just half (60 mm) is traversed by the sagitta. At injection the transverse width of the beam is largest, 25 mm, which leaves a clearance of 18 mm on both sides. The central trajectory in the magnet and the beam envelope at injection are shown in Figure 6. The clearance increases to 27 mm at 20 GeV.

Because the beam traverses 70% of the horizontal aperture, it is reasonable to raise a concern about the stability of motion of individual particles in such a configuration. Upon closer inspection, it appears that the situation is acceptable. Fermilab made measurements of the magnet field quality on centerline and at ±1, ±2 in. They show that the field is essentially flat; the gradient $(1/B)(\partial B/\partial x)$ is no more than 0.01 /m. A preliminary model of the lattice that tracks individual particles through the field suggests that the dynamic aperture is much larger than required, though this should be confirmed by more detailed studies. The magnets have also been shown to exhibit a considerable amount of remanent field. In our case, however, this does not seem to be a problem because the single-turn injection does not require a lengthy front porch, and because there is enough time between pulses to cycle the magnets in the optimal way to minimize the remanent field. Beam loss at injection is one

issue that should be addressed in more detail during the conceptual design phase, but it does not seem to be a showstopper.

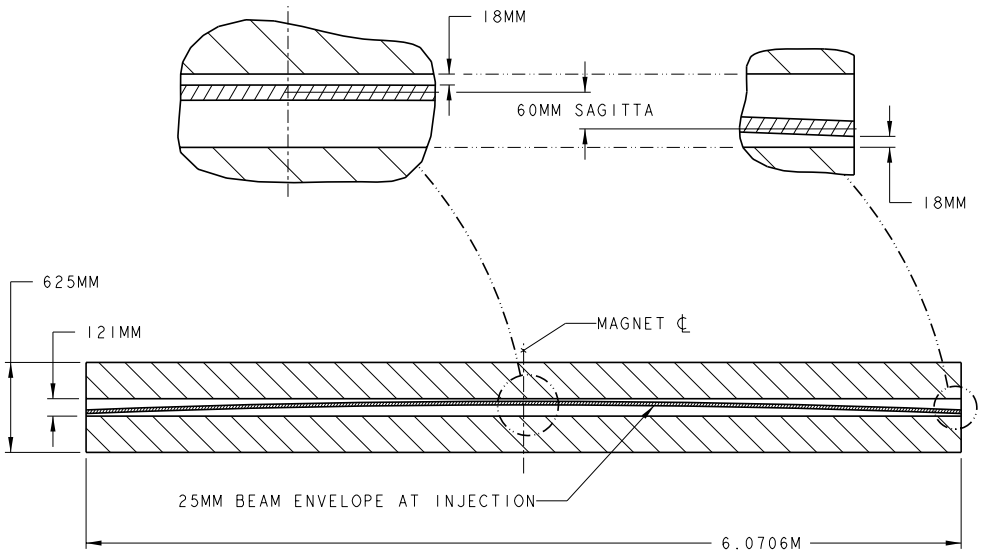

Figure 6. Reference Trajectory and Injection Beam Envelope in a Dipole.

In the vertical direction, similar considerations apply, but here there is no sagitta. The vertical physical aperture is 34 mm, while the beam full height is at most 24 mm at injection, leaving at least 5 mm clearance on top and bottom.

Quadrupole Type

The 96 quadrupoles are the Q4-type from the Main Ring, which used 240 quadrupoles.[5] Since the Scrounge-atron injects at much lower energy, it requires stronger focussing (more quadrupoles) to keep the beam size small at injection. The Main Ring used 48 Q4-type quadrupoles; approximately the same number will have to be built new, using the existing design and tooling.

Accelerator Functions

With respect to the amplitude-envelope functions, β_H and β_V, the overall periodicity is the largest possible, equal to the number of FODO cells (46). The dispersion function, η, also has a large periodicity, given by the sequence of the FODO cells in the arcs. In the insertion, the first empty cell, **CE**, and subsequent bend cell, **C**, make up a dispersion suppressor, so the dispersion is matched and nearly zero in the middle straight **CE** cell that contains the kickers. The complete matching gives a high-performance lattice with little sensitivity to magnet-to-magnet random and systematic field errors. The lattice functions are plotted in Figure 7.

Beam Parameters

The combined synchrotron beam parameters are summarized in Table 3. The second column corresponds to the injection energy value of 300 MeV, and the third column to the extraction energy of 20 GeV.

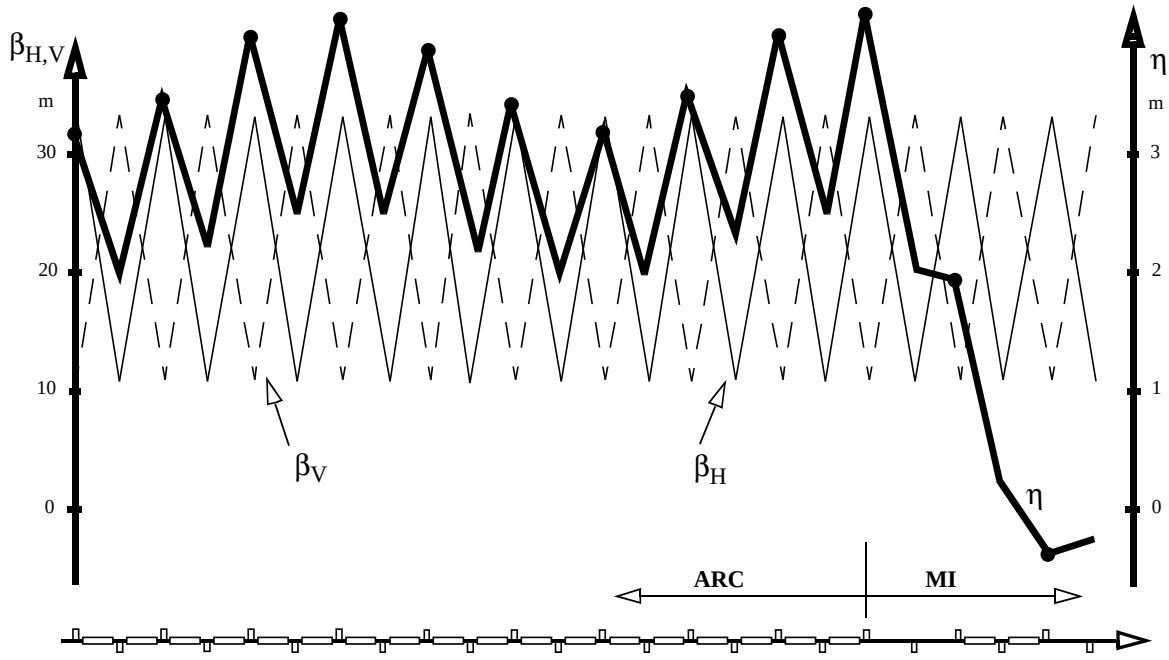

Figure 7. Lattice Functions.
Lattice functions for half a period, starting in the middle of an arc. The beam envelope functions, β_H and β_V, are plotted as thin lines against the left-hand scale; the dispersion function, η, is shown as a thick line against the right-hand scale.

Table 3 also shows the frequency range of the accelerating rf cavities, assuming an harmonic number $h = 12$. Of the 12 rf buckets, only 10 are occupied by beam bunches, which are the "frames" to be fired sequentially to the target. The beam gap created by the two missing bunches is long enough to turn off/turn on the injection and extraction kicker magnets.

Transition Crossing

The ring transition energy is $\gamma_T = 7.387$, which is encountered and crossed during the acceleration cycle. (Below the transition energy, lower-energy particles in the beam take longer to travel around the ring, since they are traveling at lower speed. As the particles become increasingly relativistic, all speeds approach the speed of light, so that above transition, higher-energy particles actually take *longer* to travel around the ring, because they travel on a longer orbit at a larger radius. At transition, since all particles take the same time to go around the ring, the rf system is unable to supply a restoring force to counter the natural growth in momentum spread. Hence, some beam loss can occur.) Transition crossing is usually seen to be a problem in high-intensity machines because of beam losses. It cannot be easily avoided without resorting to a more complicated lattice, which may require different types of magnets. However, both Fermilab (in the Booster and Main Ring) and BNL (in the AGS [Alternating Gradient Synchrotron]) have considerable experience in transition crossing with little or no beam loss, boosting confidence that the Scrounge-atron can be made to cross transition without significant beam loss. In any case, the Scrounge-atron is *not* a high-intensity machine, and therefore can tolerate modest beam losses without compromising its scientific goals.

Table 3. Energy Dependent Parameters.
Synchrotron beam parameters at injection (300 MeV) and extraction (20 GeV).

Parameter	Injection	Extraction	Units
Beam			
Kinetic Energy	0.300	20.000	GeV
Momentum	0.808	20.918	GeV/*c*
Magnetic Rigidity	26.960	697.738	kG m
Ramp Timestamp	0.174	4.514	s
B1 Type Dipoles			
Field	0.349	9.027	kG
Current	89.5	2317.2	A
Q4 Type Quadrupoles			
Gradient	2.101	54.365	kG/m
Current	38.3	991.6	A
rf Parameters			
Revolution Period	4.653	3.039	μs
rf Frequency	2.579	3.949	MHz
rf Peak Voltage	40.0	20.0	kV
rf Phase Angle	60	120	°
Emittance and Beam Size			
Emittance	4.995	0.193	π mm mrad
Beam FWHM	13.0	2.6	mm
Total Excursion	85.7	64.7	mm
Linac Pulse Sequence			
T_P, pulse length	3.790	2.291	μs
T_B, bunch length	300	11.6	ns
T_{rf}, bunch spacing	388	253	ns

Injector Linac

The injector linac delivers the required 300 MeV proton pulse structure to the ring. The injector is a sequence of accelerating structures and connecting transports, broken down as shown in Figure 8. The first section consists of a duoplasmatron H^+ ion source (IS), a low-energy beam transport (LEBT), and a radio-frequency quadrupole (RFQ), which brings the beam up to 0.75 MeV. The ion source exists and is likely available from either Fermilab or BNL. The LEBT will follow a Brookhaven National Laboratory (BNL) design. The ion source and LEBT supply continuous beam to the RFQ, which bunches and accelerates microbunches at 201.25 MHz.

Denoting by N_B the number of protons per bunch and by T_B the bunch length, the required linac peak current during a single bunch (frame) is $I_L = N_B\, e\, /\, T_B$ or 53.4 mA. Other parameters are given in Table 4. We have assumed 75% transmission through the RFQ, which yields an ion source current of 71.2 mA. The pulse duration is only 4 μs, which, at the repetition rate of one pulse per minute, gives a beam duty factor of only 6.4×10^{-6}%. We have adopted an rf duty factor of 1%, mostly for tuning of the accelerating cavities and considerably larger than the actual beam duty factor, giving an rf pulse duration of 0.6 s. These parameters represent a very modest front end, all well within the state of the art and very conservative.

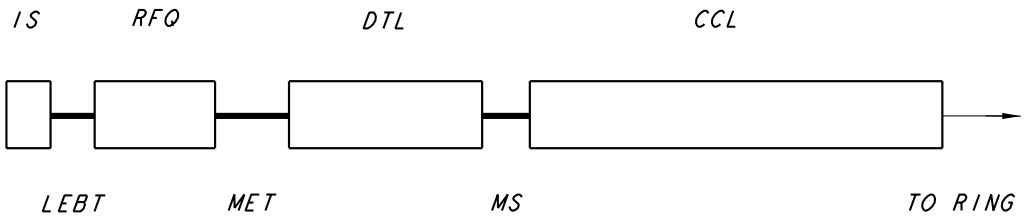

Figure 8. The Injection Linac.

Table 4. Injection Linac Parameters.

Parameter	Value	Unit
Ion Source		
Beam Pulse Duration	4	μs
Repetition Rate	1	min^{-1}
Duty Factor	6.67×10^{-5}	%
Ion Current	71.2	mA
Platform Voltage	35	kV
Emittance, full, normal	1	π mm mrad
RFQ		
Transmission	75	%
Energy	0.75	MeV
Frequency	201.25	MHz
Chopper		
Frequency	2.579	MHz
Chopping Ratio	78.2	%
DTL		
Energy	200	MeV
Frequency	201.25	MHz
Average Gradient	3	MeV/m
CCL		
Energy	300	MeV
Frequency	805	MHz
Average Gradient	3	MeV/m
Linac		
Length	100	m
Beam Peak Current (out)	53.4	mA
rf Pulse Length	0.6	s
rf Duty Factor	1	%
rf Efficiency	25	%
Momentum Spread, $(\Delta p/p)_{rms}$	0.02	%

The next major section starts with an rf chopper. The chopper kicks out microbunches from the RFQ, leaving the required 10 frames for the experiment. The chopper operates at the same rf accelerating frequency as in the synchrotron at injection. The beam pulse and the bunch-frame sequence are shown in Figure 9. T_{rf} is the rf accelerating period at injection in the ring, which also equals the chopper period. T_B is the full bunch length at injection, and T_P is the resulting linac pulse length. The beam gap duration is $T_G = hT_{rf} - T_P$, where h is the ring rf harmonic number, and T_{rf} is the rf period. The chopping ratio is 78.2%. These quantities are given in Table 4.

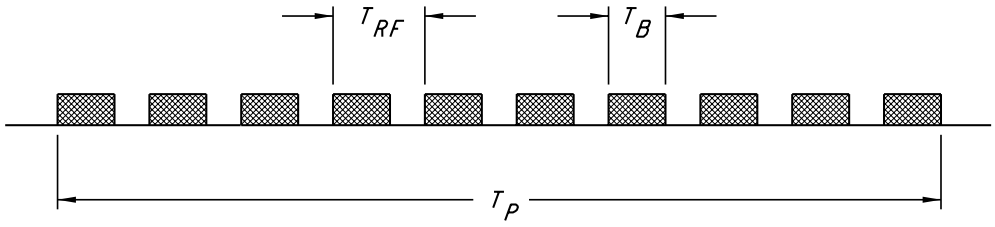

Figure 9. Beam Time Structure.
The proton beam time structure. Ten of the twelve rf buckets in the ring contain a proton bunch, which will expose a single time frame in the radiograph sequence.

Following the chopper comes the first section of drift-tube linac (DTL). This will be a copy of the BNL design and will bring the beam up to 116 MeV using 201.25 MHz rf. The next section of DTL will be the existing and decommissioned Fermilab DTL, built to the same BNL design. This will bring the beam up to 200 MeV.

Finally, the beam will enter a cavity coupled linac (CCL), based on the Fermilab design at 805 MHz, which will accelerate the beam to the final 300 MeV. The CCL section of the linac can be built from the Fermilab design.

Approximately one-third of the major linac components exist and can be scrounged—the ion source, RFQ, and second DTL section. As for the missing pieces, the first section of DTL and the CCL, the designs exist, so very little engineering design will be required.

Only one beam turn is needed to inject into the Synchrotron. The linac pulse, 4 μs long with 10^{12} protons, is injected on the fly during the ramp of the synchrotron, obviating the need for a front porch in the ring magnetic cycle.

Injection, Extraction, Transport, and Beamstops

Linac to Ring Transport

The linac to ring transport line (LTRT) takes the 300 MeV beam from the end of the linac to the injection Lambertson magnet in the synchrotron, as shown in Figure 10. Three quadrupoles, **Q1**, **Q2,** and **Q3**, follow the end of the linac for matching. The lattice of the LTRT is a natural extension of the ring lattice using three empty FODO cells ("**CE**"). A bending magnet $\mathbf{B_L}$ (1 m long, 5.4 kG) is upstream of the Lambertson at 180° horizontal phase advance to compensate for the horizontal bend of the injection Lambertson magnet. With this configuration the dispersion is matched at both ends, and the transport is achromatic.

The quadrupoles require only a modest gradient of 6 kG/m and are 50 cm long. The internal aperture is circular with an inside diameter of 10 cm. These are inexpensive magnets to build if no equivalent can be found at another site. Including the triplet at the upstream end, there are a total of 10 such quadrupoles, equipped with their own vacuum chambers, flanges, and bellows.

Vacuum pumps (six 30-liter/s ion pumps and one 600-liter/s roughing pump) and controllers can be obtained from Fermilab. Two sector valves are required, one upstream at the linac exit and the other downstream by the Lambertson magnet, to isolate the transport

line from the linac and the synchrotron, as required. Beam steering is accomplished with pairs of beam position monitors (BPMs) and dipole steering magnets (DSMs) placed at both sides of each quadrupole, for a total of seven each. The BPMs are available at Fermilab. The DSMs have to be built.

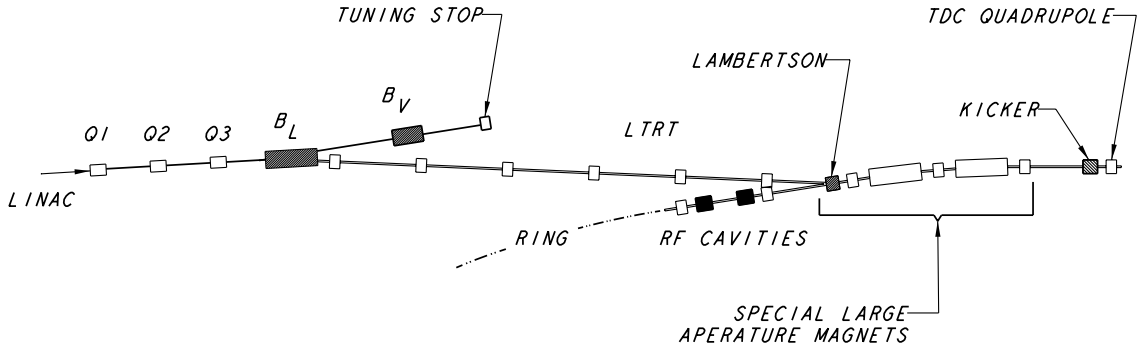

Figure 10. Linac to Ring Transport and Injection.
Proton beam transport at 300 MeV injection from the end of the linac to either the linac tune stop or the injection point in the ring. Ring injection is performed by the Lambertson and kicker.

Injection System

The injection system is made of a Lambertson magnet and a kicker magnet, located at the upstream half of the transfer middle insertion, as shown in Figure 10. The beam from the LTRT reaches the Lambertson at a 200 mr horizontal angle with respect to the axis of the **CE** cell and displaced vertically above the midplane by 50 mm. The 1 m long Lambertson magnet uses a 5.4 kG field to bend the beam horizontally by 200 mr, making the incoming beam trajectory parallel to the main orbit in the ring, but still displaced vertically above the midplane by 50 mm. The Lambertson is located 1.251 m upstream of the following quadrupole, the same distance between arc dipoles and quadrupoles. Since the injected beam is so close to the nominal orbit, the Lambertson sits on the vacuum chamber of the ring, separated by a 10 mm septum. The Lambertson physical aperture is 38 mm vertically and 127 mm horizontally.

The kicker magnet is located as shown in Figure 10 at 90^o vertical phase advance downstream from the Lambertson. The 90° phase advance brings the beam, which was initially 50 mm above the ring orbit, down onto the orbit plane, but with a downward vertical angle. The kicker removes this angle with a 2.58 mr vertical kick to complete injection. Since the cells have 60° phase advance, a 90° phase advance locates the kicker one and one-half cells after the Lambertson, 1.251 m upstream of the top dead center (TDC) quadrupole. The kicker length is 70 cm long, with a field strength of 100 G, and must turn off about 600 ns after the last bunch is injected, before the first bunch has come all the way around the ring. The internal physical aperture is 38 mm vertically and 127 mm horizontally.

To allow sufficient space for both the circulating and injected beams, special large-aperture magnets (2 dipoles and 3 quadrupoles) will have to be built, along with the Lambertson and kicker magnets.

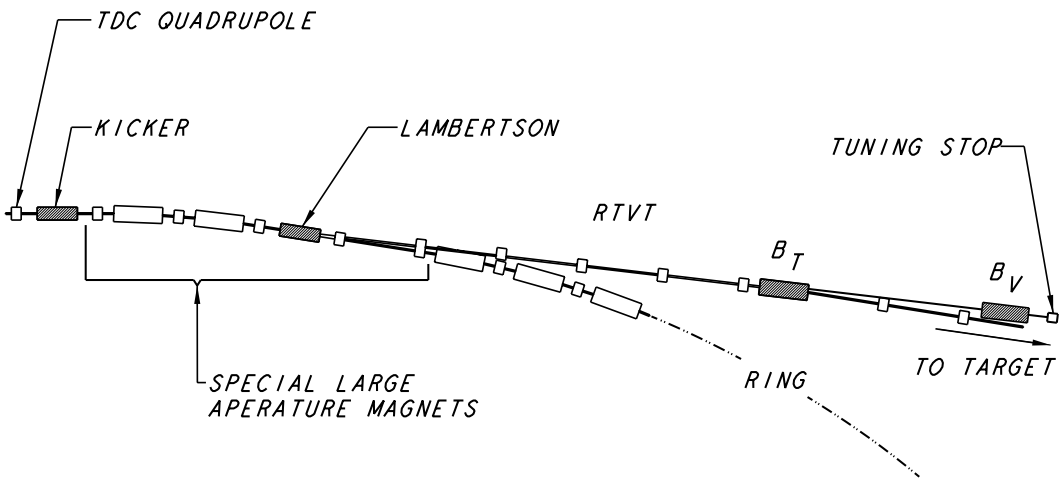

Figure 11. Extraction and Extraction Transport Line.
Proton beam transport at 20 GeV from the ring extraction to either the ring tuning stop or the radiography beamline. Ring extraction is performed by the kicker and Lambertson. The TDC quadrupole is the rightmost magnet in Figure 10.

Extraction System

Extraction is also done in a single turn using longer and stronger Lambertson and kicker magnets. The circulating beam is first kicked vertically downward by 2.58 mrad by the kicker magnet. After 90° phase advance, the beam is displaced vertically down by 50 mm when it reaches the entrance of the Lambertson magnet, as shown in Figure 11. The Lambertson magnet then bends the beam horizontally by 42 mr away from the ring. As for the injection magnets, the spacing between the extraction Lambertson and kicker magnets and the adjacent quadrupoles is 1.251 m.

The Lambertson is 6 m long with a field strength of 4.9 kG. It sits below the B1-type vacuum chamber of the ring, separated by a septum 10 mm thick. The internal physical aperture is 38 mm vertically and 127 mm horizontally. The kicker magnet is also 6 m long, with the same physical aperture as the Lambertson magnet. The required field strength is 300 G, which has to turn on in 400 ns during the beam gap between the last bunch and the first.

To allow sufficient space for both the circulating and injected beams, special large-aperture magnets (2 dipoles and 5 quadrupoles) will have to be built, along with the Lambertson and kicker magnets.

Ring to Radiography Transport

The transport line that takes the 20 GeV beam from the ring to the radiography beamline (RTRT) is a natural extension of the ring lattice. A bending magnet $\mathbf{B_T}$ is located at 180° horizontal phase advance downstream of the extraction Lambertson to compensate for the horizontal bend of the Lambertson magnet. The magnet is a B1-type Fermilab dipole with a field of 4.9 kG. The three cells between the Lambertson and $\mathbf{B_T}$ contain four Q4 quadrupoles (as well as two of the large-aperture quadrupoles mentioned above).

This section will require six 30 liter/s ion pumps, one 600 liter/s roughing pump, and sector valves at each end, as in the LTRT. As in the LTRT, beam steering is accomplished with pairs of beam position monitors (BPMs) and dipole steering magnets (DSMs) placed at both sides of each quadrupole, for a total of seven each. The BPMs are available at Fermilab; the DSMs have to be built.

The transport from the vacuum interruption after $\mathbf{B_T}$ to the diffuser, which starts the radiography beamline, consists of a multiple of 3 **CE** cells, each of which provides a unit inverting transfer matrix. This is a modular approach and simplifies the matching. Each three cell unit requires six 30 liter/s ion pumps; 600 liter/s roughing pumps are also required in the area. Some beam steering is required, using the same components as above. The target area beamline has a separate vacuum from the ring, so that any potential failures of the blast protection do not vent the entire ring. The end of the $\mathbf{B_T}$ vacuum chamber marks the interface between the ring vacuum and the target vacuum.

Beamstops and Abort System

For linac and ring tuning it will be necessary to dispose of the beam in a controlled fashion without sending it to the radiography area. Two beamstops are located in the transfer gallery, one for the linac and one for the ring, as shown in Figure 10 and Figure 11. In the case of the linac, the $\mathbf{B_L}$ magnet is used as a switch magnet. For linac tuning the magnet is off, which allows the beam to travel to the $\mathbf{B_V}$ dipole, where it is bent vertically down toward the beam stop, a block of iron buried in the ground. The $\mathbf{B_V}$ dipole could be a B2-type Fermilab dipole (if available), which is always on. The switch magnet $\mathbf{B_L}$ is turned off between linac pulses as a precaution. Assuming that the full-intensity 300-MeV beam is dumped, the peak power is 15 MW during the 4 μs pulse length. Given a repetition rate of one pulse per minute, the average power is only 1 W.

The abort system monitors operation of the ring for excessive radiation levels, power supply failures, or other faults during the ramp cycle. If a fault is detected, the abort system triggers immediate extraction of the beam to one of the dumps. During ring tuning the $\mathbf{B_T}$ magnet is turned off, so that the beam continues straight until it is bent vertically down by the $\mathbf{B_V}$ magnet toward the beam stop. To allow aborts at any time, the $\mathbf{B_V}$ dipole field tracks the beam momentum. The $\mathbf{B_V}$ dipole could also be a B2-type Fermilab dipole (if available). During radiography tuning and running the beam enters an identical beam stop at the end of the radiography beamline, at the right in Figure 12. Again, to enable aborts at any time, the $\mathbf{B_T}$ magnet tracks the beam momentum. For either mode, dumping the full-intensity 20 GeV beam puts an average 60 W power into the beamstop.

Since the dynamic experiments need only a few μs from trigger to detonation, the firing signal can require a "good beam" input during the last few turns around the ring. This means that extractions initiated by the abort system will not result in premature radiographs of the dynamic experiment.

Radiography Beamline

The radiography beamline provides the beam distribution to illuminate the object and produce images necessary for radiographic analysis. The main elements of the beamline are the diffuser, the matching lens, and a series of three identical imaging lenses, as illustrated in Figure 12.

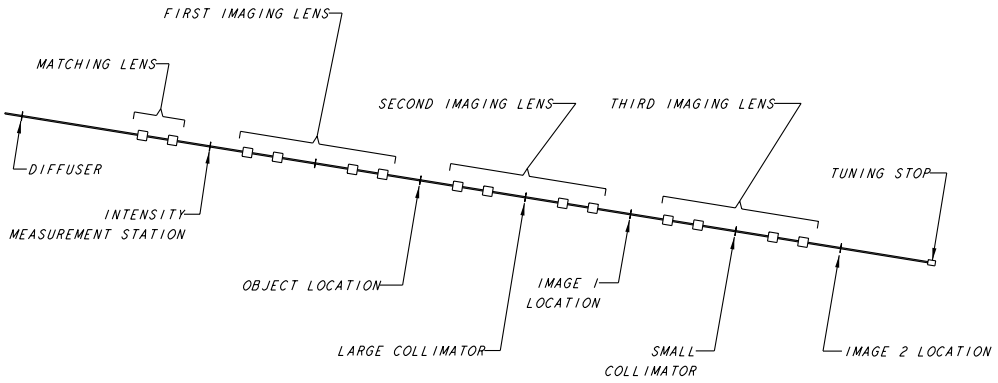

Figure 12. Radiography Beamline from Diffuser to Beam Stop.

The diffuser is a piece of material of sufficient thickness to provide an enlarged beam illumination. The diffuser may be a set of plates of varying thicknesses which can be selectively driven into the beam to provide various illumination profiles. The matching lens sets up a relationship between a beam particle's radial distance from the beamline and its slope. This relationship is such that at least part of the first-order achromaticity of the imaging lenses is canceled. The distance from the diffuser to the matching lens is set by the matching condition.

The matching lens consists of a pair of quadrupole magnets. An imaging station, referred to as I_0, provides information on the illuminating beam distribution. This imaging station allows images from each pulse to be normalized with the actual incident flux, significantly relaxing any flux stability requirement on the accelerator. The accelerator need not have constant, or even stable, flux on a pulse-by-pulse or shot-to-shot basis since all of the flux distributions are measured. If the I_0 imaging detector system is identical to the other detectors and the alignment of the detectors is within one resolution pixel, then it is possible to achieve a reduction in the statistical fluctuations of the images.

The first imaging lens transports the I_0 beam image onto the object. This lens is composed of two quadrupole doublets. The characteristics of these lenses have been discussed previously. The lens located after the object transports the surviving beam to the I_1 station. A third lens transports the beam to the final imaging system I_2. Differences in collimation in the second and third lenses provide information that allows material identification in the object.

All of the magnets and power supplies are standard equipment that can be found at BNL. Most are currently used in the E933 Proton Radiography Experiment. If this equipment is not available for use at the Scrounge-atron, the equipment can be reproduced.

Magnet System

Dipole Magnets

As already discussed, the Scrounge-atron uses B1-type dipoles because of their larger horizontal aperture. Approximately 270 dipoles are available. The dipoles have three coils, which create a minor field asymmetry. To compensate, the magnets were built in two subtypes—with the third coil up (above the beam pipe) or with the third coil down. The two subtypes should alternate with each other in the **C** cells.

Quadrupole Magnets

The Main Ring was made of 192 Q7-type quadrupoles (84 in. = 2.134 m long) and 48 Q4-type quadrupoles (52 in. = 1.321 m long).[5] Our first choice would be the Q7-type because enough of them already exist. Unfortunately, almost all of these magnets have become part of the Main Injector, leaving essentially none available for the Scrounge-atron. We have therefore designed around the Q4-type, though only 48 exist, and at least as many have to be built new. Apart from the different length, both types of quadrupoles have the same physical aperture of 5×2 in.^{2} = 127×51 mm^2. For the Scrounge-atron lattice with Q4-type quadrupoles the gradient needed is 54 kG/m at 20 GeV, which is about half of the Main Ring gradient at 200 GeV.

Main Magnet Power Supplies

Table 5 summarizes the electrical parameters of the ring dipoles and quadrupoles at 20 GeV. All the dipole magnets will be powered in series on the same power supply bus. The quadrupole magnets of each family (`QF` and `QD`) will be connected in series on the same power supply bus, but independent from each other to allow easy tuning operation.

Table 5. Dipole and Quadrupole Electrical Properties.
Electrical properties of the B1-type dipoles and Q4-type quadrupoles at 20 GeV. The duty cycle assumes a constant ramp rate, both up and down, from Table 2**;** the peak field, from Table 3; and the repetition rate from Table 4**.** The total number of magnets is shown in Table 6. The total supply voltage is per power supply, not the total voltage around the ring.

Parameter	**B1 Dipole**	**Q4 Quad.**	**Unit**
Peak Field or Gradient	9.027	54.365	kG or kG/m
Peak Current	2317	992	A
Resistance	5.92	2.90	mΩ
Inductance	6.47		mH
Peak Voltage	13.72	2.88	V
Peak Power	31.788	2.852	kW
Duty Factor	15	15	%
Average Power	1.594	0.143	kW
Stored Energy	34.741		kJ
Total Number	84	110	
Number in Ring	80	92	
# of Power Supplies	6	2	
Magnets per PS	13.3	46	
Totals			
Peak Power	2.670	0.314	MW
Average Power	134	15.7	kW
Supply Voltage	182.9	132.3	V
Stored Energy	2.918		MJ

The power supply arrangement is shown in Figure 13.[6] The dipole current and the two quadrupole currents flow in opposite directions to cancel the magnetic fields generated by the bus current. The dipoles are connected in series by 6 power supply stations, which are located in the power supply utility buildings. Each family of quadrupoles is connected in series to a single power supply placed in separate utility buildings. The ring is served by a

total of 8 power supplies; two more are required for each of the transport lines, for a total of 10 power supplies and substations. Each power supply station requires six phases of AC from delta- and wye-connected transformers. The 13.8 kV power line enters each of these substations through a manual disconnect, vacuum breaker, and the delta- and wye-connected transformers. Most of this equipment is available from Fermilab.

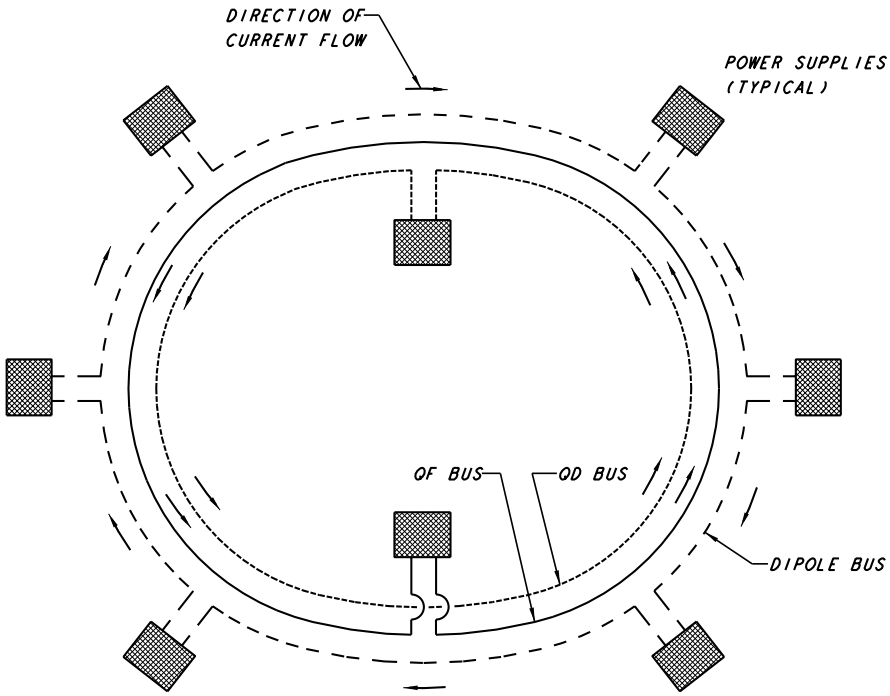

Figure 13. Ring Power Supply Busing.

The AC power is rectified and controlled locally by a computer that generates the linear ramp. From practically zero field, the magnets are ramped at 2 kG/s. After 175 ms when the field reaches 350 G, the beam is injected in a single turn on the fly (without halting the field ramp). Acceleration of the beam continues to 20 GeV as the field ramps to 9 kG, which takes 4.325 s. The beam is immediately extracted, again on the fly in a single turn. Following extraction the field is ramped down in a programmed manner to reduce the effects of the remanent field at injection on the next cycle. The total magnet cycle takes 9 s.

This is a much simpler magnet cycle than used in the Main Ring.[3] There, the 200 GeV cycle was typically 6–10 s long, starting with a 0.8 s front porch to inject multiple booster batches. The accelerating ramp took about 1.5 seconds at 6 kG/s, followed by a 2–4 s flattop for resonant extraction. Finally, the guiding field was ramped down at 6 kG/s, and the cycle repeated. The absence of a front porch in the Scrounge-atron cycle makes the injection process less sensitive to magnetic field errors, which are the primary concern in operating at low injection field.

The low repetition rate and short ramp result in low average-power consumption. The water pressure required to cool the magnets so that the temperature of the coils does not change by more than 20 ^{o}C is correspondingly modest, 0.0007 psi, assuming a magnet duty factor of 5%. This suggests that water cooling may not be necessary as long there is equivalent air flow in the ring tunnel.

Magnet Raft

The Q4 quadrupoles, all correcting elements, and beam monitors are mounted on a strongback, the magnet raft, as in the Main Injector. The arrangement of elements is sketched in Figure 14. The raft simplifies installation in the tunnel since all components are pre-mounted and aligned to the raft. Once mounted in the tunnel, the raft itself is aligned. If the tolerance stack up is excessive, the individual component positions can be checked by the survey team and adjusted, as necessary.

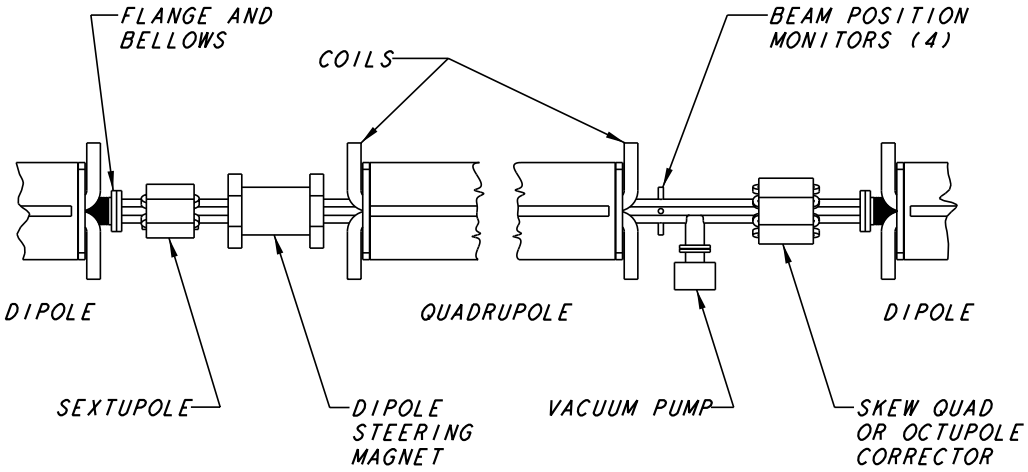

Figure 14. Magnet Raft Components.

Beam Steering

Beam Steering is accomplished with dipole steering magnets (DSMs) and adjacent beam position monitors (BPMs) that read the beam center position, either horizontal or vertical. These components are shown in Figure 14. The DSMs are located next to the Q4 quadrupole magnets; the BPMs are integrated into the quadrupole vacuum pipe. There are two families of BPM and DSM paired together—those operating on the horizontal plane, placed next to the `QF` quads, and those operating on the vertical plane, placed next to the `QD` quads. The BPM are pairs of striplines cut diagonally with a total length of about 30 cm. The low-level electronic signal is collected individually and transferred to the control room for processing. The DSMs are individually powered and have iron cores 30 cm long, providing fields of a few hundred Gauss. The current is set from the control room after processing the BPM reading. All the DSM will have to be built to the Fermilab design with existing tooling.

Sextupole Magnets

The sextupole magnets are also iron-core magnets of 30 cm length, which are available from Fermilab. They are used to correct sextupole component field errors and, if desired, to offset the ring natural chromaticity. They are placed next to each quadrupole, as shown in Figure 14. These are powered in two families: `SF` next to `QF` and `SD` next to `QD`. The Fermilab sextupole magnets use 25.4 mm spacers on the midplane to create a dodecapole field, which conveniently compensates for a nonlinearity of the same shape in the dipole remanent field. Since the Scrounge-atron has four times as many sextupoles (one per dipole) as the Main Ring, this spacer will have to be changed to the appropriate thickness.

Other Corrector Magnets

Higher-order correcting magnets are also used. These include 24 skew quadrupoles, each about 20 cm in length, and 24 octupoles of the same length. These two systems will be powered in four or six groups and adjusted from the control room.

Quantities and Availability

The total number of magnets of each type required for the LTRT, ring, RTRT, and radiography line are tabulated in Table 6. All the dipoles exist and are available. Approximately 40% of the quadrupoles exist and are available; the remainder have to be built using the Fermilab design and tooling. All the corrector magnets exist, except for the DSM. The various large-aperture and special magnets (Lambertsons, kickers) will probably be built new, based wherever possible on existing designs.

Table 6. Magnet Types and Quantities.
Number of each type of magnet required, by location. "LA" refers to special large-aperture magnets used in injection, extraction, and the radiography line. "Available" magnets are available at Fermilab; "To Build" will be built to existing Fermilab designs using existing tooling.

Type	Required	Available	To Build
Dipoles			
B1 Dipoles	**84**	**270**	
Ring	80		
LTRT: B_L, B_V	2		
RTRT: B_T, B_V	2		
Ring LA Dipoles	**4**		**4**
Lambertsons	**2**		**2**
Kickers	**2**		**2**
Steering Dipoles	**116**		**116**
LTRT	6		
Ring	92		
RTRT	18		
Quadrupoles			
LTRT Quads	**6**		**6**
Q4 Quadrupoles	**110**	**40**	**70**
Ring	92		
RTRT	18		
Ring LA Quads	**8**		**8**
Radiography LA Quadrupoles	**14**		**14**
Correctors			
Skew Quadrupoles	**24**	**24**	
Sextupoles	**80**	**80**	
Octupoles	**24**	**24**	

Other Systems

rf Cavities

Acceleration is provided by the rf cavities, which are programmed to follow the magnetic field ramp. At a harmonic number, *h*, of 12, 40 kV peak rf voltage is required both for acceleration and to provide a large enough rf bucket for the 0.2 eV s beam bunch. The fixed rf parameters are given in Table 7; the energy dependent parameters at injection and extraction are shown in Table 8. The required frequency range is narrow and similar to several other operating systems. The power demand is also modest.

Table 7. Fixed rf Parameters.

Parameter	**Value**	**Units**
Harmonic Number	12	
Acceleration Period	4.514	s
Repetition Rate	1	min^{-1}
Duty Factor	7.523	%
Field Ramp	2.000	kG/s
Cavity Length	1.8	m
Cavity Diameter	0.8	m
# of Cavities	3	
# of Gaps per Cavity	2	

Table 8. Varying rf Parameters at Injection and Extraction.

Parameter	**Injection**	**Extraction**	**Units**
rf Frequency	2.579	3.949	MHz
rf Peak Voltage	40.0	20.0	kV
rf Phase Angle	60	120	°
Peak Voltage per Cavity	13.3	6.67	kV
Average Beam Current	34.4	52.7	mA
Peak Beam Power	1.19	0.913	kW
Dissipated Power per Cavity	20	5	kW
Bunch Area, Full	0.2	0.4	eV s
Bucket Area	0.4	0.8	eV s
Bunch Height, $(\Delta p/p)_{rms}$	0.05	0.01	%
Bucket Height, $(\Delta p/p)$	0.15	0.04	%

To supply this accelerating voltage, three of the four existing Princeton-Penn Accelerator (PPA) cavity assemblies,[7] which are now unused at Fermilab, will be located at the upstream end of the transfer insertion, before the injection kicker, as shown in Figure 10. The cavities are in very good condition, needing only minor refurbishment and small modifications. The power amplifiers and drivers are also available. The only major missing component is the ferrite bias bus bar and bias current power supply, but the requirements are modest. In addition, the complete rf system requires low-level feedback loops to lock the rf to the beam bunch phase and radial signals. These are also relatively simple.

Vacuum

The vacuum system is largely the Main Ring system, obtained from Fermilab.[8] The vacuum chambers, with 1.25 mm stainless steel walls, are epoxied into the dipoles and quadrupoles. Most of the original bellows at the ends of the dipoles have been cut, so they will be replaced with new bellows and flanges. The **D** drifts between the dipoles and quadrupoles will be made from the Main Ring short drift beam pipes. The corrector magnets bolt around this pipe; they need no vacuum pipes of their own.

Rough pumping will be done with four 600 l/s oil diffusion pumps and mechanical backing pumps. The ring will be broken into six vacuum sectors (half of each arc and the two insertions), as well as the LTRT and RTRT vacuum sectors. The roughing pumps and sector valves are available at Fermilab. A 30 l/s sputter ion pump is located at each Q4 quadrupole. These pumps are all available, including power supplies. A gas chemical analyzer will be required as a diagnostic tool.

Using essentially the same pumping per unit length, the Main Ring achieved 5×10^{-8} torr. After roughing out, the Main Ring maintained this vacuum using the ion pumps only; no additional roughing was required. It remains to verify that 5×10^{-8} torr is adequate for 300 MeV operation. The same pressure in the Main Ring allowed operation at 8 GeV.

Instrumentation

The beam position monitors, used in tandem with the DSMs, are integrated into the quadrupole vacuum pipes. There are other necessary beam diagnostic devices which are not available from Fermilab, because they have gone into the Main Injector, such as beam profile monitors, beam wall monitors, bunch length detectors, pingers, and rf knockout electrodes. A broadband pickup device, generally made of striplines, is also useful in combination with a frequency analyzer. Transverse and longitudinal beam dampers are also needed and will be developed as part of the rf system.

Controls and Operations

There are a number of good existing models for the control system, either home-grown, as at Fermilab, BNL, or LANL, or commercial (BridgeView). The Scrounge-atron presents no novel issues from the controls standpoint. A typical system has acquisition computers located in the service buildings that collect and preprocess signals from the diagnostic sensors. This data is then forwarded to a central computer system at the control room for archive and display. A number of consoles display performance measures for the various subsystems.

The operations mode is likely to differ significantly from most operating accelerators. Scrounge-atron operations may be fairly episodic, with beam required only during the day for a brief run. This schedule will be driven by the experimental program. Typically the experiments may require one week of beam to set up the detectors and object for a particular dynamic experiment. After some experiments, a significant period (days) may be required for cleanup before the next experiment can be mounted. This pattern suggests that beam may only run during the days, with the machine in a “warm standby” mode overnight. Between runs, the machine may go to a complete stand down, with only housekeeping functions, such as vacuum pumps, running. Start up operations will be significantly simplified if the machine can be brought up quickly at the start of a run. This will be facilitated by a powerful control system that assists operators in understanding the machine behavior at a high level.

Civil Engineering, Enclosures, and Radiation Shielding

The general requirements for the enclosure are that it should be wide enough for the ring and a magnet mover and tall enough for workers to walk upright. It should have cable trays and a communications antenna, as used in all modern occupied tunnels. In addition, periodic pipe support fixtures are required to support the magnet buses and LCW (low-conductivity water) loops. All areas should be equipped with lights, emergency lights, utility power, fire-pull stations and annunciators. While some moisture incursion can be tolerated, the magnets and bus bars should not be directly exposed to water. The tunnel environment should be protected from extremes of temperature and humidity.

The Main Ring was originally commissioned without the LCW system operational, using a low-power ramp cycle. The machine was ramped to 50 GeV at the nominal repetition rate, with a full energy (200 GeV) ramp every few minutes. This operation mode was sufficient for much of the initial machine tuning, without overheating the magnets. In the Scrounge-atron, a reduced power cycle might consist of ramps to 5 GeV every minute, with a 20 GeV ramp approximately every five minutes. Using the planned cycle, or a reduced power cycle, preliminary calculations suggest that the Scrounge-atron could operate without water cooling, using either free or forced convection, with acceptable steady state magnet temperatures. If this preliminary work is borne out by detailed modeling, the Scrounge-atron could operate without water in the magnets. This would eliminate the dominant cause of magnet failures in the Main Ring. Cooling water will be required in the linac and for specific devices in the ring, such as the injection, extraction, and rf systems, and likely the buses.

Preliminary radiation shielding calculations indicate that little, if any, earth cover is required to attenuate the radiation levels from the ring. Simple scaling with energy and intensity from the Fermilab Main Ring (6 m) or Main Injector (7 m) shielding would indicate that ~0.5 m is sufficient. An alternative to the Fermilab completely buried design is to locate the magnets slightly below grade, and use the excavated material to build a small berm *outside* the ring. This creates a radiation shadow beyond the berm; at a modest distance, the radiation field is at sufficient height that personnel or material at ground level are unaffected. A fence would restrict access to the area immediately adjacent to the berm where the shadow is less than ~3 m high. These estimates are preliminary; complete modeling, using a code such as `CASIM`, and regulatory approval of the accident scenarios will be required during the civil design phase.

As for construction techniques, commercial culvert sections, either precast concrete or corrugated steel, have been used elsewhere. Big cost savings can be realized by using local industrial capabilities, *i.e.*, adopting the design of the local sewer culvert, for which local cement contractors already have forms. Figure 15 shows a typical configuration, using corrugated steel sections, welded together and resting on a reinforced concrete pad.

The linac enclosure is likely to be of more conventional construction. Cost savings can be realized by locating the power amplifiers as close to the linac as possible, but outside the radiation enclosure. Typically this goal has been met by constructing two parallel galleries separated by a shielding wall, as shown schematically at the top left in Figure 3.

Firing Point

The experimental program requires a site capable of open air firing of high explosives, such as BEEF (Big Explosive Experiment Facility)[9] at the Nevada Test Site. Locating the Scrounge-atron firing point at the existing BEEF would realize cost savings in firing table, firing control, bunkers, muster areas, explosives handling, *etc*. To allow

nonradiographic experiments to continue at BEEF, the radiography beamline is located below grade. The Scrounge-atron firing point would be in a pit, offset from the main BEEF firing point. This layout, sketched in Figure 16, has the pit displaced towards the get-lost dump. For non-radiographic tests, the pit is covered by blast protection (cement blocks, overlain by gravel). For radiographic tests, the pit is uncovered, and the test object located at the firing position. The proton beam would leave the vacuum of the underground beamline through a window in the blast shield bull nose, traverse the firing pit and object, then pass through a second window at the other side of the pit and into the imaging beamline. Although it is desirable to design the windows to survive the blast, failures have only a modest impact on operations. Since the beamline vacuum is separated from the ring vacuum at the vacuum interruption point, failure of the firing point windows will vent only the beamline, not the entire machine.

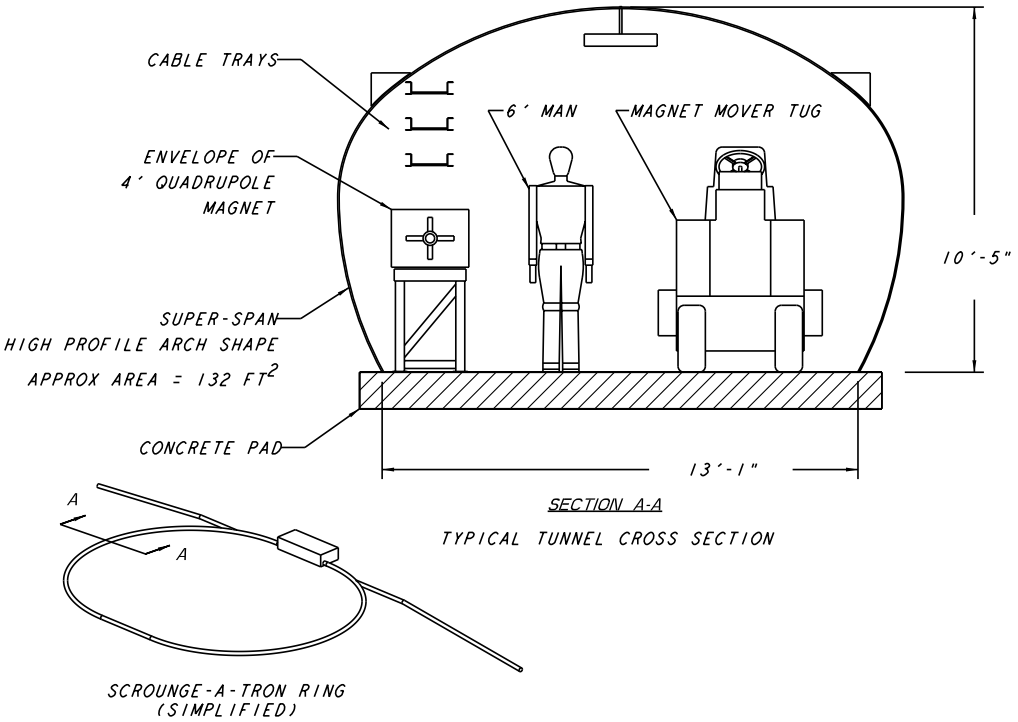

Figure 15. Scrounge-atron Enclosure.

Power Requirements

Table 9 shows the peak and average power requirements, based on the linac operation parameters in Table 4 and a ring ramp rate of 2 kG/s up and down. We have assumed a 1% duty factor for the linac rf. To take into account the power dissipated in the cavities in absence of a detailed design of the Linac, we have also assumed a 25% overall rf efficiency, which includes the AC-to-rf conversion efficiency. A repetition rate of 1 ppm has also been assumed. The bottom line is that the total peak power requirement is under 100 MW, with an average power consumption of around 7.5 MW.

Scrounging Fermilab

Table 6 lists the quantity of each type of magnet required, along with the number available from Fermilab and the number that will have to be built from existing Fermilab

designs. Many other components are potentially available at Fermilab, such as magnet power supplies, corrector elements, beam diagnostic equipment and electronics, interlocks and other low-level controls. Whether a given component from Fermilab is actually used will depend on its condition, the extent of refurbishment or modification required, and the cost of providing that function from new designs and hardware.

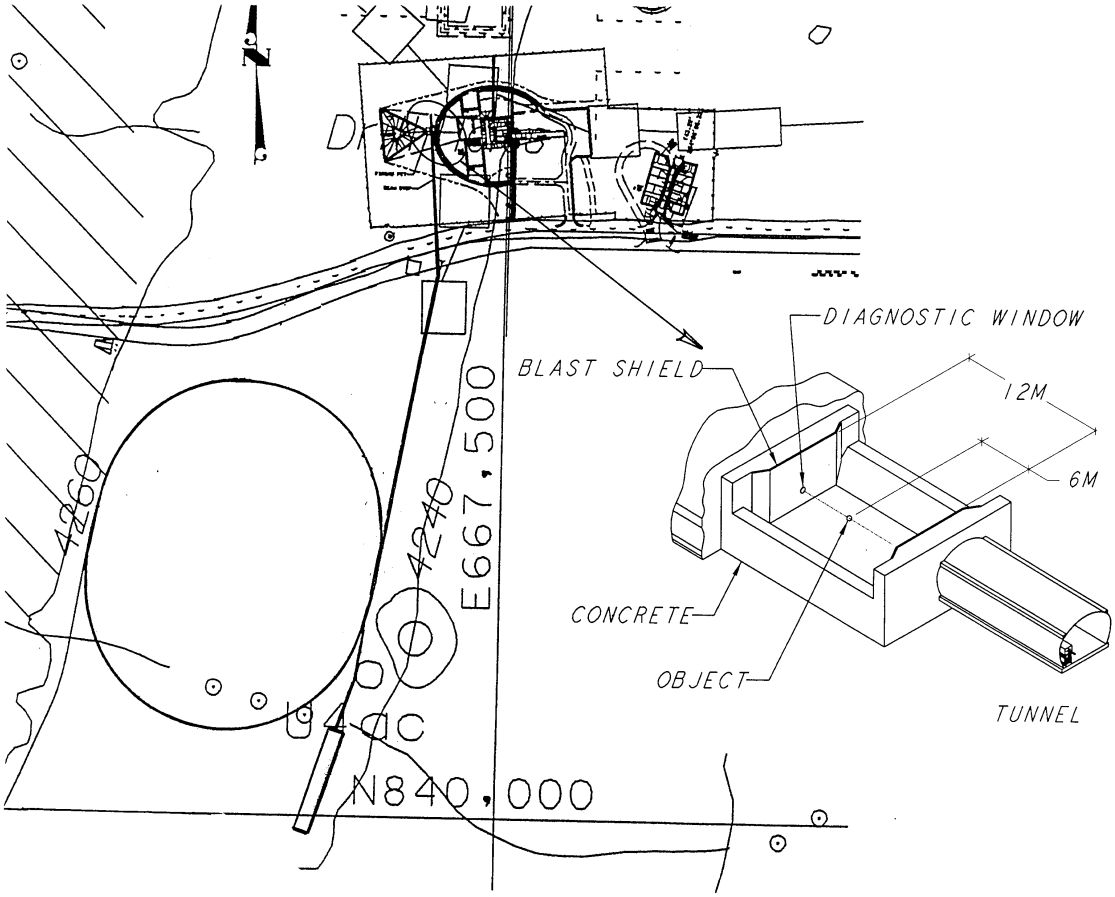

Figure 16. Scrounge-atron at BEEF.
Possible layout of the Scrounge-atron at BEEF in the Nevada Test Site. The injector and accelerator ring are shown to scale. In this layout the ring is the mirror image of that shown in Figure 3. The inset shows a concept for the firing pit.

Schedule

Figure 17 shows a technically driven schedule, based on a top-down analysis. The Scrounge-atron can be built in three years. This schedule makes a number of assumptions: the machine design has already been frozen during the preparation of a Conceptual Design Report (CDR) or Technical Design Report, the site has been selected, and any required approval process has been completed. Resource constraints are not included.

Table 9. Site-wide Power Requirements.
Site-wide power requirements, based on the operation cycle listed in Table 1 and Table 5.

System	Duty Factor	Power (MW)	
	(%)	Average	Peak
Linac		**0.641**	**80.10**
Beam	6.7E-05	0.000	16.02
rf	1	0.641	64.08
LTRT	100	**0.300**	**0.30**
Ring		**1.591**	**4.78**
Magnets	15	0.449	2.98
Instrumentation	100	0.100	0.10
Vacuum	100	0.200	0.20
rf System	7.5	0.023	0.30
Injection	5	0.005	0.10
Extraction	5	0.015	0.30
Control	100	0.300	0.30
Air Cooling	100	0.500	0.50
RTRT	1	**0.003**	**0.30**
Radiography Beamline	100	**2.000**	**2.00**
Site General	100	**3.000**	**3.00**
Grand Total		**7.541**	**91.1**

The critical path is driven by the civil construction. The civil construction start date depends on two activities—freezing the civil requirements and obtaining approval and funding for construction. The civil requirements depend on the basic machine design, such as length of the linac, ring, and beamlines. Therefore, it is very important to freeze the basic machine design as early as possible. The most likely civil construction funding path will require Congressional line-item approval. This takes about two years to secure and depends critically on submission of the CDR, by approximately April, for inclusion in the DOE budget request for the fiscal year beginning 18 months later. Missing this date forces the funding into the subsequent fiscal year, adding one year to the schedule.

Cost

A work breakdown structure (WBS) and top-down cost estimate are shown in Table 10. These are based on a model WBS to level 4 in most cases and do not include contingency. One of the two main cost drivers is the linac. The other main driver is the civil construction. Since the bulk of the ring technical components have been identified, the ring cost is quite small, around $10 M.

Several different cost models have been analyzed, particularly for the linac and the civil construction options. The results have been consistent within 20%. Because of the coarse nature of this analysis, a 50–100% contingency should be used at this stage, mostly assigned to the linac and civil parts of the project. For the linac, since the designs exist and most (if not all) components have been built once, it should be possible to develop relatively quickly a detailed and robust cost estimate with modest contingency. Since the linac uses proven designs, the risks will be small. The situation for the civil construction is similar. Freezing the machine design will allow detailed and accurate cost estimates based on trade studies and analysis of construction options.

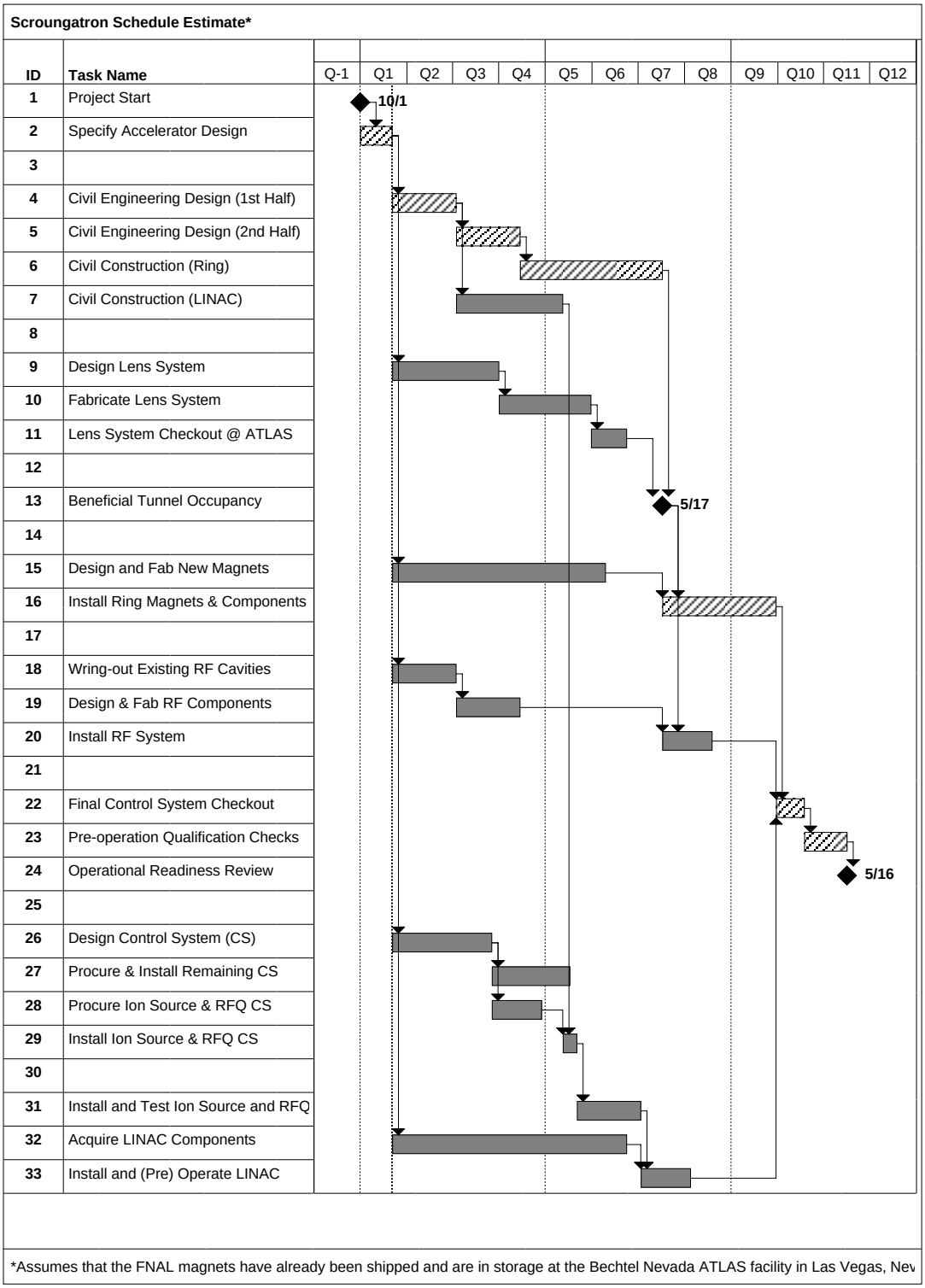

Figure 17. Technically Driven Construction Schedule.

The key to meeting a low budget target with low contingency is preventing the technical design specification from straying significantly from the baseline. This requires a strong management able to resist the inevitable pressure to increase the scope. Any additional technical information produced from added features and capabilities may not outweigh the time and cost penalty incurred in delaying the completion of the machine. Further, building a

technically advanced machine at some level works against the concept of a phased approach to the AHF.

Table 10. Work Breakdown Structure and Cost Estimate.

WBS #	Item	Cost ($K)
0	**Project total**	**$75,006**
1	**Physics & Management**	**$4,564**
2	**Accelerator**	**$54,493**
2.1	Injector	$33,975
2.1.1	Ion source	$148
2.1.2	Low energy transport	$87
2.1.3	RFQ	$2,400
2.1.4	Medium energy transport	$142
2.1.5	Drift tube linac to 116 MeV	$10,618
2.1.6	Drift tube linac to 200 MeV	$10,618
2.1.7	Drift tube linac to 300 MeV	$8,363
2.1.8	Local linac control	$1,600
2.2	Synchrotron	$14,644
2.2.1	Magnet system	$10,141
2.2.2	Magnet power system	$1,880
2.2.3	Ring vacuum system	$1,024
2.2.4	rf system	$796
2.2.5	Beam diagnostics	$4
2.2.6	Local Ring Control System	$800
2.3	Transfer lines and dumps	$4,073
2.3.1	Linac-to-ring transport	$1,140
2.3.2	Linac beam dump	$257
2.3.3	Injection System	$280
2.3.4	Extraction system	$420
2.3.5	Ring to vacuum break transport	$938
2.3.6	Ring beam dump	$257
2.3.7	Vacuum break to diffuser transport	$782
2.4	Master controls	$1,800
2.4.1	Consoles and operation system	$600
2.4.2	Timing and coordination	$600
2.4.3	Safety and interlocks	$600
3	**Target Area**	**$4,130**
3.1	Firing Table	$35
3.2	Imaging system	$3,990
3.3	vacuum	$35
3.4	Instrumentation	$35
3.5	Beam diagnostics	$35
4	**Conventional construction**	**$11,820**
4.1	Site preparation	$180
4.2	Linac	$1,200
4.3	Ring	$5,460
4.4	Transfer lines	$2,400
4.5	Special underground structures	$720
4.6	Buildings	$600
4.7	Primary power	$700
4.8	Mechanical systems	$560

Energy, Intensity, and Beamline Upgrades

Energy Upgrade

The synchrotron described here is certainly capable of operating at higher energy. The Main Ring routinely operated at 400 GeV (17.9 kG) and briefly at 500 GeV (21.5 kG). The corresponding fields in the Scrounge-atron will result in 40 GeV and 50 GeV operation, respectively. Operation of the Main Ring at 500 GeV was limited by two factors: the two families of dipoles, B1 and B2, have different saturation behavior, making tuning difficult; and the power company could not sustain the load. Since the Scrounge-atron uses only the B1 dipoles, tuning issues should be significantly simpler, even at 50 GeV. The power will increase significantly, from 5 MW to 20 MW peak in the ring; the average power will increase from 1.5 MW to 7 MW in the ring.

Other parameters that depend on the top energy are shown in Table 11. These assume that the ramp duration is fixed at 4.325 s and the beam intensity is fixed at 10^{12} protons per pulse. The excitation current increases linearly with momentum, except at the highest momentum where saturation effects are becoming significant; the corresponding power increases quadratically. One possible limitation to the energy may be the extraction kicker and Lambertson magnets. The fields shown in Table 11 assume a fixed 6 m length. These fields are challenging though still technically feasible. The higher energy may also necessitate more radiation shielding, which can be achieved by adding material to a berm.

Table 11. Energy Upgrade Parameters.

Parameter	Top Energy			Units
	20 GeV	40 GeV	50 GeV	
Beam				
Momentum	20.918	40.928	50.930	GeV/*c*
Magnetic Rigidity	698	1365	1699	kG m
B1 Type Dipoles				
Field	9.027	17.663	21.979	kG
Current	2317	4534	5642	A
Field Ramp Rate	2.257	4.416	5.495	kG/s
Q4 Type Quadrupoles				
Gradient	54.37	106.4	132.4	kG/m
Current	992	1940	2414	A
Ring Power				
Peak	4.78	13.22	19.49	MW
Average	1.59	4.53	7.65	MW
rf				
Injection V_{peak}	40	40	50	kV
Extraction V_{peak}	20	40	50	kV
Beam Peak Power	0.913	0.914	0.914	kW
Total rf Power	40	40	50	kW
Extraction				
Kicker Field	0.300	0.587	0.730	kG
Lambertson Field	4.900	9.587	11.930	kG

Intensity Upgrade

As discussed on p. 8, the intensity limit of the Scrounge-atron is set by the space-charge limit. In that calculation we made the conservative assumption that a tune shift of $\Delta\nu = 0.2$ is acceptable. In fact, it may very well be possible to operate the ring with a tune shift larger by as much as a factor of two. For the same beam emittance, this would allow a factor of two increase in the intensity.

Further increases in the intensity require injecting at higher energy. According to the $\beta^2\gamma^3$ factor, injecting at 1.25 GeV gives an order of magnitude intensity gain. This could be accomplished by inserting a small, rapid-cycling booster between the linac and the ring, as sketched in Figure 18. The booster would accelerate one beam bunch at a time by accumulating five bunches from the linac, which would need modest upgrades to increase the bunch charge by two. Each booster bunch would be injected into the ring in boxcar fashion during a "front porch" in the field ramp. If the booster cycle frequency is 15 Hz, such as the FNAL Booster, the ring will hold at the 850 G injection field for 0.7 s before beginning to accelerate the ten bunches.

Due to the higher injection energy, the injection Lambertson and kicker may have to be replaced with higher field or longer versions. At higher intensity and higher energy (40-50 GeV) the beam power becomes comparable to the dissipated rf power, which may necessitate more cavities. Radiation shielding requirements will also increase. The ultimate intensity limit will probably come from the negative mass instability encountered in crossing transition.

(Nearly) Arbitrary Pulse Formats

The least demanding extraction scheme has already been described—all ten bunches extracted during a single turn. This fixes the time between bunches, or frames, at 253 ns. A kicker with a 200 ns fall time (or rise time) would provide considerable flexibility. With such a kicker it would be possible to extract a single bunch at a time, leaving the remainder in the ring. On a subsequent turn, a second bunch could be extracted to provide a second frame, and so on for the remaining bunches. If all frames are extracted in a modest number of turns, no flattop is required; each bunch will have slightly more energy than the previous one. To achieve this flexibility, the kicker will have to have a short enough rise (or fall) time. This scheme also requires a set of modulators connected in parallel to the kicker. Each modulator has to be capable of kicking out one beam pulse without setting off the others. This would allow the experimenter to place the ten frames in any pattern desired, modulo the 3.0 μs revolution time and 253 ns bunch spacing, over a total duration easily as long as a fraction of a second.

Beamline Upgrade to the AHF

The Scrounge-atron was originally envisioned as a demonstration machine that would not attempt to meet the full AHF requirements. In fact, it appears that Scrounge-atron could become the injector to a complete AHF. A concept is sketched in Figure 18. The basic principle is to inject three consecutive Scrounge-atron pulses into a fixed-energy collector ring. At this point, the three sets of ten bunches are extracted simultaneously along three arms. Along each arm, each bunch would be split twice, resulting in 10 bunches traveling down each of twelve beamlines. Since each bunch would have nominally 1/4 of the initial bunch charge, the Scrounge-atron would be augmented by a 1.25 GeV booster ring, resulting

in 2.5×10^{11} protons per axis per frame at the object. The collector ring and beamlines could be built from the remaining FNAL B1 dipoles; all the quadrupoles would have to be built new.

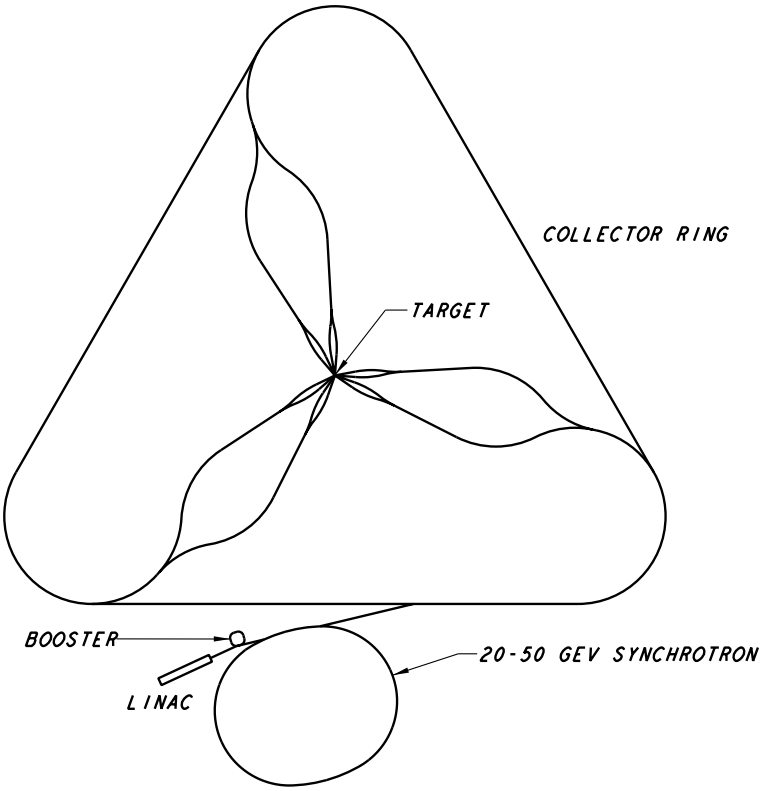

Figure 18. Scrounge-atron and the AHF.
Sketch of the Scrounge-atron as the injector to a 12-axis proton AHF. Three pulses from the Scrounge-atron would be accumulated in the collector ring, then extracted along three arms simultaneously. Each arm would split the beam bunches twice, resulting in twelve beams on the target.

Recommendations for Future Work

Considering its nature, this exploratory research is by no means meant to be a proposal for construction. Though the results are definitely encouraging and no showstoppers have been found, this work has been done in a short period of time and with limited effort. A more detailed study leading to a conceptual design report should be undertaken. There are a relatively few areas where concentrated effort would have significant impact in reducing the cost and schedule uncertainty. On the technical side, these are:

- Further develop the linac cost and schedule. Also consider a 12 MeV linac feeding a rapid-cycling booster with a peak energy of 300 MeV or 1.25 GeV.

- Develop the magnet skid assembly, which integrates the scrounged components into the basic repeated element of the ring.

- Evaluate the operation of the existing PPA rf cavities to prove they can provide the required accelerating voltage.

On the project management side, effort should be focused on:

- Conventional construction concepts trade-off study.

On the accelerator physics side, the only significant issue is

- Dynamic aperture at injection due to remanent field errors, alignment, and sagitta.

Conclusion

The result of this Exploratory Research is that an accelerator built from exiting parts is technically feasible and can be built for less than $100 M within three years. To meet the schedule and cost goals, this machine relies heavily on the availability of components from the decommissioned Fermi National Accelerator Laboratory (Fermilab) Main Ring as well as the other accelerator laboratories. The driving principle of the Scrounge-atron, to use existing parts where available and appropriate, or to use existing designs, or, lastly to design the required parts, is a viable approach for the creation of a proton accelerator to demonstrate proton radiography. This approach minimizes the total amount of design for the accelerator and is possible because the characteristics required for radiography are far below the current state-of-the-art of existing accelerators.

The decommissioning of the Fermilab Main Ring has made a large variety of parts available for reuse. The cost of building these parts new may only represent on the order of 10% of the total cost. However, the reuse of these parts reduces the machine design and construction schedule significantly. This is important in providing a timely demonstration of proton radiography as a technology to be considered for the AHF.

We have also shown that there is a natural upgrade path from the Scrounge-atron to a full AHF. It is possible with only minor modifications to accelerate and extract the proton beam at 50 GeV, if this should be required. With a more advanced kicker magnet it will be possible to extract one proton bunch at a time and achieve a nearly arbitrary frame spacing over a much longer time interval. The addition of a small rapid-cycling booster will increase the proton beam intensity by an order of magnitude, if this should be required. A large external collector ring increases the intensity and adds the capability to simultaneously extract several beam bunches along multiple axes.

To summarize, it is possible to build the Scrounge-atron as a demonstration accelerator for proton radiography, with a 20 GeV beam of ten pulses, 10^{11} protons each, spaced 250 ns apart, delivered once a minute to a single-axis radiographic station centered at the BEEF facility of the Nevada Test Site. These parameters are sufficient to demonstrate, in five years, the capabilities of a proton-based Advanced Hydrotest Facility. The Scrounge-atron can be built in two to three years for less then $100 million, by using components from the decommissioned Fermilab Main Ring. Finally, the Scrounge-atron will begin returning valuable science many years earlier and at a fraction of the initial cost of the full AHF.

References

1. Final Programmatic Environmental Impact Statement for Stockpile Stewardship and Management, DOE-EIS-0236 (U. S. Department of Energy, 1996).

2. A. Gavron, *et al.*, Proton Radiography, LA-UR-96-420 (Los Alamos National Laboratory, 1996).

3. E. Malamud, Status of the 500 GeV Accelerator, in proceedings of the 1971 Particle Accelerator Conference, Chicago, IL, 1-3 March 1971, IEEE Transactions on Nuclear Science, **18**, 948.

4. H. Hinterberger, *et al*., Bending Magnets of the NAL Main Accelerator, in proceedings of 1971 Particle Accelerator Conference, Chicago, IL, 1-3 March 1971, IEEE Transactions on Nuclear Science, **18**, 853.

5. H. Hinterberger, *et al*., Quadrupole Magnets of the NAL Main Accelerator, in proceedings of 1971 Particle Accelerator Conference, Chicago, IL, 1-3 March 1971, IEEE Transactions on Nuclear Science, **18**, 857.

6. R. Cassel and H. Pfeffer, The Power Supply System, Control, and Response of the NAL Main Accelerator, in proceedings of the 1971 Particle Accelerator Conference, Chicago, IL, 1-3 March 1971, IEEE Transactions on Nuclear Science, **18**, 860.

7. J. L. Kirchgessner, *et al*., The RF System for the Princeton-Pennsylvania Accelerator, IRE Trans. on Nuclear Science **NS-9**, 2, 11 (1962).

8. Main Ring Rookie Book, April 10, 1991 (Fermi National Accelerator Laboratory, 1991).

9. A. Davito, *et al*., POPOVER Review Panel Report, UCRL-ID-123426 (Lawrence Livermore National Laboratory, 1996).